

Document de travail (Docweb) n°2212

## **The Risk of Inflation Dispersion in the Euro Area**

Stéphane Lhuissier, Banque de France

Aymeric Ortmans, Université Paris-Saclay, Univ Evry, EPEE

Fabien Tripier, Université Paris Dauphine, Université PSL, LEDa CEPREMAP

Novembre 2022

# Le risque de dispersion des taux d'inflation en zone euro <sup>1</sup>

Stéphane Lhuissier<sup>2</sup>, Aymeric Ortman<sup>3</sup>, Fabien Tripier<sup>4</sup>

**Résumé :** Cet article étudie la divergence au cours du temps des distributions prédictives de l'inflation dans les pays de la zone euro et explore ses déterminants macroéconomiques. Alors que la dispersion des taux d'inflation concerne principalement les risques d'inflation à la hausse durant la première décennie de la zone euro, elle s'est déplacée vers les risques d'inflation à la baisse durant la deuxième décennie. La dispersion des risques d'inflation à la baisse et à la hausse a atteint des niveaux record à la suite de la crise du COVID. Les tensions financières constituent le principal déterminant des risques d'inflation à la baisse. Dans le prolongement de la crise du COVID, ce sont principalement les pressions sur les chaînes de valeur qui ont entraîné la dispersion des risques d'inflation à la hausse. Dans l'ensemble, la dispersion des taux d'inflation est largement due à l'hétérogénéité des courbes de Phillips entre les pays plutôt qu'à des contextes économiques nationaux différents.

**Mots-clés :** Inflation ; Risque d'inflation ; Dispersion de l'inflation ; Union monétaire ; Zone euro

## The Risk of Inflation Dispersion in the Euro Area

**Abstract :** We document the time-varying divergence of predictive inflation distributions across euro area countries and explore their macroeconomic origins. While the dispersion of inflation rates mainly concerns upside inflation risks during the first decade of the euro area, it shifted to downside inflation risks during the second decade. The dispersion of downside and upside risks to inflation reaches record levels in the wake of the COVID crisis. The main determinant of the dispersion at the bottom of the distribution is the development of financial stress. In the wake of the COVID crisis, value chain pressures drove the dispersion of upside inflation risks. Overall, the dispersion of inflation rates is largely caused by heterogeneous Phillips curves between countries rather than by different national economic contexts.

**Keywords :** : Inflation; Inflation-at-Risk; Inflation dispersion; Monetary Union; Euro area

---

<sup>1</sup>Fabien Tripier acknowledges financial support from the French ANR (DEMUR research project ANR-20-CE26-0013), and from CEPREMAP

<sup>2</sup>Banque de France, 31, Rue Croix des Petits Champs, DGSEI-DEMFI-POMONE 41-1422, 75049 Paris Cedex 01, FRANCE (Email: stephane.lhuissier@hotmail.com; URL: <http://www.stephanelhuissier.eu>). The views expressed in this paper are those of the authors and should under no circumstances be interpreted as reflecting those of the Banque de France or the Eurosystem

<sup>3</sup>Université Paris-Saclay, Univ Evry, EPEE, 91025, Evry-Courcouronnes, France Sciences Po (Email: [aymeric.ortmans@universite-paris-saclay.fr](mailto:aymeric.ortmans@universite-paris-saclay.fr))

<sup>4</sup>Université Paris Dauphine, Université PSL, CNRS, IRD, 75016 PARIS, FRANCE CEPREMAP (Email: [fabien.tripier@dauphine.psl.eu](mailto:fabien.tripier@dauphine.psl.eu)).

## I. INTRODUCTION

Our objective in this paper is to document the time-varying divergence in the predictive inflation distributions across euro area countries and explore their macroeconomic origins. Fluctuations in the dispersion of the *conditional mean* of inflation between countries over time are a well-known phenomenon. Average inflation differentials between countries show a clear cyclical pattern, rising sharply in economic downturns and falling in booms, as shown in Figure 1. The literature has been widely devoted to studying the key drivers behind these cross-country differences. By contrast, the study of the divergences in the *tails* of the inflation distribution remains completely unexplored. Yet, the dispersion of inflation in the euro area (both headline and core) appears to be more pronounced in the tails of the distribution than in the middle, as shown in Table I. The (unconditional) standard deviation across countries of inflation (both headline and core) tends to be two to three times higher in the 10<sup>th</sup> and 90<sup>th</sup> quantiles than that in the median. In this paper, we aim at providing a more complete picture of inflation differentials across euro area countries by delivering measures of inflation dispersion over time associated to the different quantiles of the predictive inflation distributions, and at identifying their main drivers.

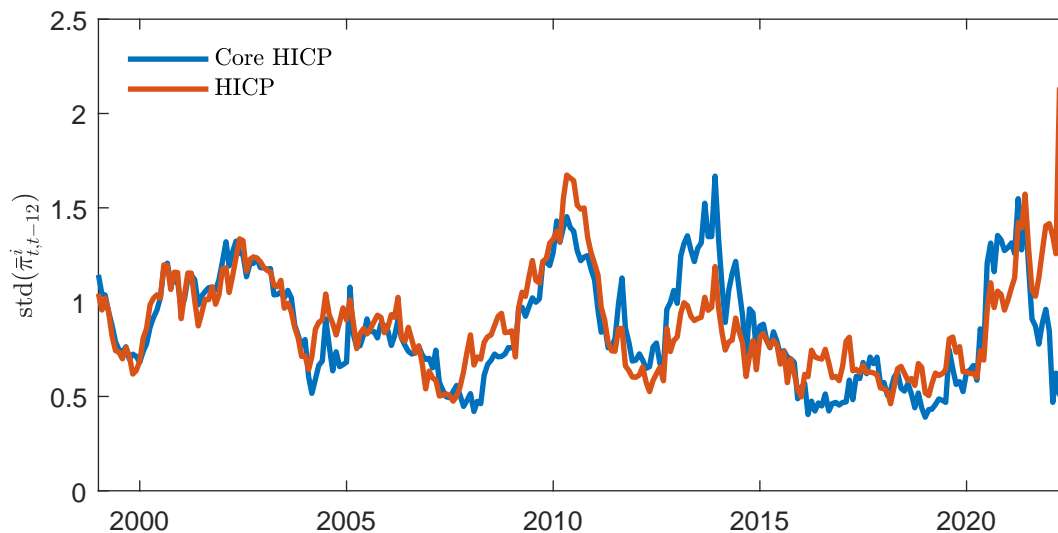
Our approach builds on the concept of inflation-at-risk developed by [Andrade et al. \(2014\)](#), [Banerjee et al. \(2020\)](#), and [López-Salido and Loria \(2022\)](#), which is itself highly related to that of Growth-at-Risk developed by [Adrian, Boyarchenko, and Giannone \(2019\)](#).<sup>1</sup> Inflation-at-risk approach aims at forecasting shifts in the tails of inflation distribution. [López-Salido and Loria \(2022\)](#) provide an in-depth analysis of inflation-at-risk in the euro area and the U.S. grounded on a quantile Phillips curve. Here, we are not interested in the inflation risk for one country *per se*, but in the dispersion of these inflation risks between euro area countries.

The literature on inflation-at-risk is relatively silent when it comes to the analysis of this risk of inflation dispersion. However, as for inflation itself, it is critical for the policy maker to know what type of tail risks (upside or downside) are causing the dispersion of inflation especially in a monetary union. The conduct of a single monetary policy, with a common inflation target, is indeed more difficult if countries have diverging inflation rates. Countries with high inflation differentials will suffer from inappropriate monetary policy

---

<sup>1</sup>See also [Plagborg-Møller et al. \(2020\)](#) and [Figueres and Jarociński \(2020\)](#) for an application to the euro area.

FIGURE 1. Cross-sectional standard deviation of inflation rates in the euro area



*Note:*  $\bar{\pi}_{t,t-12}^i$  denotes the average over the last 12 months of the monthly inflation rate (core and headline inflation rates, annualized) for the country  $i$  of the euro area (12 countries, fixed composition, Austria, Belgium, Finland, France, Germany, Greece, Ireland, Italy, Luxembourg, Netherlands, Portugal, Spain). The sample is January 1999 to July 2022. The figure shows the cross-country unweighted standard deviation of annual inflation rates in the euro area. See Section A in the online appendix for data description.

decisions with respect to their specific economic context. Inflation dispersion at the bottom of the inflation distribution exposes diverging economies to the risk of costly deflation due to nominal downward rigidity while at the top of the distribution, diverging economies are exposed to the risk of inflationary spirals.

To elaborate our measure of risk of inflation dispersion, we proceed as follows. Firstly, we estimate a quantile Phillips curve based on [López-Salido and Loria \(2022\)](#) for each euro area country and not for the euro area as a whole as done by these authors. We can then compute the predictive inflation distributions by country. Conditional quantiles vary over time according to the evolution of key economic and financial variables included in the Phillips curve (namely, past and expected inflation rates, unemployment gap, financial stress, oil inflation, and supply chain pressures). Secondly, for each date, we compute the standard deviation across these national quantiles of inflation. By looking at the different quantiles of the inflation distribution, we can evaluate the cross-country dispersion of the inflation-at-risk at the bottom of the distribution (i.e. the risk of low inflation or deflation) and at the top

TABLE I. Moments of inflation by country

	Core HICP				HICP			
	Mean	Median	10 <sup>th</sup>	90 <sup>th</sup>	Mean	Median	10 <sup>th</sup>	90 <sup>th</sup>
Germany	1.19	1.10	0.43	2.06	1.63	1.44	0.33	3.16
France	1.18	1.16	0.53	1.87	1.62	1.50	0.66	2.72
Italy	1.70	1.76	0.68	2.64	1.73	1.75	0.28	3.16
Spain	1.65	1.70	0.24	3.01	2.16	2.00	-0.12	4.67
Netherlands	1.63	1.41	0.60	2.91	2.04	1.75	0.44	3.98
Finland	1.37	1.30	0.47	2.37	1.68	1.48	0.28	3.31
Ireland	1.46	1.43	-0.89	3.86	1.73	1.61	-0.87	4.53
Austria	1.76	1.69	1.07	2.56	1.94	1.78	0.73	3.36
Portugal	1.57	1.45	-0.03	3.36	1.87	1.73	-0.12	4.06
Belgium	1.77	1.68	1.19	2.45	1.97	1.92	0.61	3.43
Luxembourg	1.74	1.70	1.12	2.41	2.45	2.32	0.67	4.43
Greece	1.33	1.47	-1.22	3.70	1.95	1.79	-0.87	4.99
Mean	1.53	1.49	0.35	2.77	1.90	1.75	0.17	3.82
Std. Dev.	0.22	0.22	0.75	0.62	0.25	0.25	0.56	0.72

*Note:* Mean, median, 10<sup>th</sup> and 90<sup>th</sup> quantiles for each country of the euro area (12 countries, fixed composition: Austria, Belgium, Finland, France, Germany, Greece, Ireland, Italy, Luxembourg, Netherlands, Portugal, Spain). The sample is January 1999 to July 2022. The last two rows are the unweighted means and the standard deviations of moments across countries. See Section A in the online appendix for data description.

of the distribution (i.e. the risk of excessive inflation). Third, we investigate the drivers of inflation dispersion by considering various scenarios regarding the national economic series and the structure of the Phillips curve.

We apply this framework to a euro area made from its first 12 member countries (Austria, Belgium, Finland, France, Germany, Greece<sup>2</sup>, Ireland, Italy, Luxembourg, Netherlands, Portugal, Spain). We restrict ourselves to this euro area with fixed composition to avoid the dispersion of inflation rates that would result from changes in the composition of the euro

<sup>2</sup>We include Greece in our sample even though it officially adopted the euro in 2001, two years after its creation.

area due to the more recent entry of countries. The analysis is done for the period starting in January 1999, at the creation of the euro, to July 2022. Our main results are as follows.

- (1) There has been a shift in the nature of inflation dispersion in the euro area. While the dispersion of inflation rates mainly concerns the top of the distribution during the first decade of the euro area, it shifted to the bottom of the distribution during the second decade of the euro area.
- (2) The dispersion of inflation-at-risk reaches record levels in the wake of the COVID crisis, a period marked by international tensions on energy prices and supply chains.
- (3) The main determinant of this dispersion at the bottom of the distribution was the evolution of financial stress associated with the financial and sovereign debt crisis.
- (4) In the wake of the COVID crisis, value chain pressures drove the dispersion of inflation at the top of the distribution.
- (5) Overall, the dispersion of inflation rates is largely caused by heterogeneous Phillips curves between countries rather than by different national economic contexts.

**Relation to other studies.** Our paper contributes to the literature on inflation dynamics in the euro area context. We contribute to the literature on inflation dispersion, which has been a long-standing issue in the European Monetary Union. Inflation dispersion was an important issue in defining the ECB's strategy at its inception, see [Issing et al. \(2003\)](#), as well as in its recent strategy review in 2021 as discussed in depth by [Consolo et al. \(2021\)](#) and [Reichlin et al. \(2021\)](#). It is also worth mentioning that inflation differentials per se may not be detrimental to the monetary union if they reflect the process of nominal convergence and economic development catch up. That being said, as highlighted by the [ECB \(2005\)](#), it is necessary to assess the underlying causes of inflation differentials observed at the early stage of the euro area to formulate the most appropriate monetary policy response.<sup>3</sup> Inflation differentials in the euro area has also been discussed in the academic literature. [Angeloni and Ehrmann \(2007\)](#) investigate the sources of euro area inflation differentials from 1998 to 2003. As a result, they identify that demand shocks have been the main source of inflation differentials in the early years of the EMU, followed by cost-push shocks and exchange rate

---

<sup>3</sup>[Cœuré \(2019\)](#) underlines how the ECB has always found a way to deal with the heterogeneity that could have impaired the transmission of monetary policy across euro area countries.

shocks. [Beck, Hubrich, and Marcellino \(2009\)](#) decompose regional inflation rates into a common area-wide, a country-specific and an idiosyncratic regional component. They warn of the potential high welfare costs that may represent inflation differentials fueled by national economic distortions. [Estrada, Galí, and López-Salido \(2013\)](#) explore the role of EMU in inflation convergence/divergence among euro area countries. Despite persistent inflation differentials in the euro area, they do find any critical role for the EMU in inflation convergence in the euro area. [Haan \(2010\)](#) offers a survey of this abundant literature subsequent to the creation of the euro area. We revisit this literature by providing a more complete picture of inflation differentials across euro area countries through measures of inflation dispersion associated to the different quantiles of the predictive inflation distributions.

We also contribute to the literature on the estimation of the Phillips curve. Since recent debates have focused on the death (and the revival) of the Phillips curve, and especially in the U.S. (see [Blanchard, Cerutti, and Summers \(2015\)](#), [Coibion and Gorodnichenko \(2015\)](#), [Coibion, Gorodnichenko, and Ulate \(2019\)](#), [Del Negro et al. \(2020\)](#) and [Hazell et al. \(2022\)](#), among others), little recent evidence has been put forward regarding the Phillips curve in the euro area. Importantly, and in line with our paper, [Ball and Mazumder \(2021\)](#) focus on an estimated Phillips curve using euro area core inflation. Their results suggest a non-negligible role of inflation expectations and output gap in driving core inflation fluctuations in the euro area. [Eser et al. \(2020\)](#) give a broad picture of the implication of the Phillips curve analysis in the euro area for the conduct of ECB's monetary policy. The article of this literature that is closest to ours is [López-Salido and Loria \(2022\)](#) who bring to this Phillips curve literature the quantile analysis to highlight the role of financial conditions in the downside risk to inflation. Our contribution to this literature is to elaborate cross-country measures of risk dispersion. Using national data of euro area members, we show that there are contrasting responses to economic and financial variables between the inflation tails and median.

The rest of the paper is organized as follows. Section [II](#) describes the empirical strategy to estimate the inflation-at-risk by country and then compute measures of inflation-at-risk dispersion. Section [III](#) examines the evolution of the risk of inflation dispersion in the euro area. Section [IV](#) discusses the drivers of inflation dispersion. Section [V](#) conducts robustness checks by performing a Markov-switching approach. Section [VI](#) concludes.

## II. EMPIRICAL STRATEGY

In the existing literature, the study of the determinants of cross-country dispersion of the conditional mean of inflation has been an important step to assess the relevance of regional divergence within the euro area for economic policies and the single monetary policy. To provide a more complete picture, we examine the entire inflation distribution, with a particular focus on the response of the tails of the predictive inflation distribution to economic and financial developments.

This section presents the general methodology employed in this paper. Section II.1 discusses the baseline statistical model in which conditional inflation quantiles are expressed as a function of economic and financial conditions for each country. By doing so, we are able to study the reaction of each quantile of the distribution of future inflation as a function of the state of the economy, with a particular focus on lower and higher quantiles. Section II.2 shows how to use the quantiles to approximate the entire inflation distribution using a flexible yet parametric specification. This allows us to capture the first four moments and to show probability density functions. Finally, Section II.3 describes our different measures of cross-country dispersion of inflation risks.

We use augmented quantile Phillips curve models along the lines of López-Salido and Loria (2022) to examine the effects of different factors on inflation differentials across euro area countries. That is, we extend the model by incorporating a measure of global supply chain pressure to take into account supply chain disruptions that have harmed the global economy since the start of the COVID-19 pandemic. Many commentators have perceived such disruptions as having been a key driver of the rise and fall of inflation over the recent period. Once our augmented model is estimated for each country, we are able to deliver measures of cross-country inflation dispersion over time associated to the different quantiles of inflation distribution. By doing so, we test the role of different risk factors on the inflation differentials of mean versus the tail risks of the inflation distributions.

**II.1. Phillips Curve Quantile Regressions.** We rely on quantile regression models for studying the determinants of cross-country dispersion of the entire distribution of inflation. Let us denote by  $\bar{\pi}_{t+1,t+h}^i$  the annualized average growth rate of core Harmonized Index



of Consumer Prices (HICP) between  $t + 1$  and  $t + h$  for country  $i$ , and by  $x_t^i$  a  $1 \times k$ -dimensional vector containing the conditioning variables for country  $i$ , including a constant. Our benchmark for the horizon is  $h = 12$ , that is the average inflation over the next year.

Following [López-Salido and Loria \(2022\)](#), we consider a linear model for the conditional inflation quantiles whose predicted value:

$$\hat{Q}_\tau(\bar{\pi}_{t+1,t+h}^i | x_t^i) = x_t^i \hat{\beta}_\tau^i, \quad (1)$$

is a consistent linear estimator of the quantile function of  $\bar{\pi}_{t+1,t+h}^i$  conditional on  $x_t^i$ ; where  $\tau \in (0, 1)$ ,  $\hat{\beta}_\tau^i$  is a  $k \times 1$ -dimensional vector of estimated quantile-specific parameters.

Our model for conditional inflation quantile augments the Phillips curve model used in the literature as follows:

$$\begin{aligned} \hat{Q}_\tau(\bar{\pi}_{t+1,t+h}^i | x_t^i) = & \hat{\mu}_\tau^i + (1 - \hat{\lambda}_\tau^i) \pi_{t-1}^{*,i} + \hat{\lambda}_\tau^i \pi^{LTE,i} + \hat{\theta}_\tau^i (u_t^i - u_t^{*,i}) + \\ & \hat{\gamma}_\tau^i (\pi_t^{o,*} - \pi_t^{*,i}) + \hat{\delta}_\tau^i f_t^i + \hat{\phi}_\tau^i sc_t, \end{aligned} \quad (2)$$

where all variables are monthly time series covering January 1999 through July 2022. Data sources are presented in [Appendix A](#).

The variables  $\pi_{t-1}^{*,i}$  and  $\pi_t^{LTE,i}$  represent average inflation over the previous twelve months and a measure of long-term inflation expectations, respectively. The relative importance of both variables is determined by the parameter  $\lambda_\tau^i$ . We impose  $(1 - \lambda_\tau^i) + \lambda_\tau^i = 1, 0 \leq (1 - \lambda_\tau^i) \leq 1$  and  $0 \leq \lambda_\tau^i \leq 1$ , as in [Blanchard, Cerutti, and Summers \(2015\)](#) and [López-Salido and Loria \(2022\)](#)<sup>4</sup>, using the inequality constrained quantile regression method developed by [Koenker and Ng \(2005\)](#). We use six- to ten-year-ahead inflation expectations from Consensus Economics as long-term inflation expectation series.

Our second risk factor is the unemployment gap measured as the difference between the unemployment rate  $u_t^i$  and the natural rate of unemployment  $u_t^{*,i}$ , which is obtained by applying the HP filter to the unemployment rate with the smoothing parameter equal to 14,400. The parameter  $\theta_\tau^i$  captures the slope of the Phillips curve at various inflation quantiles. Following [Blanchard, Cerutti, and Summers \(2015\)](#), we impose  $\theta_\tau^i \leq 0$ .

The third risk factor  $\pi_t^{o,*} - \pi_t^{*,i}$  represents variations in relative oil price, where  $\pi_t^{o,*}$  is the average inflation over the previous twelve months of crude oil price. This allows to

---

<sup>4</sup>[Hazell et al. \(2022\)](#) impose  $\lambda = 1$  to estimate U.S. regional Phillips curve.

capture the pass-through of oil prices into core inflation measures.<sup>5</sup> The literature provides mixed evidence of the role of energy price and import prices as a key inflation determinant. For instance, [Kilian and Zhou \(2021\)](#) find that gasoline prices do not explain the improved fit of the Phillips curve augmented by household inflation expectations during the years that followed the Great Recession. On the other hand, [Matheson and Stavrev \(2013\)](#) find an increasing importance of import-price in explaining inflation fluctuations, while [Salisu, Ademuyiwa, and Isah \(2018\)](#) point a better forecast performance when including oil prices into the Phillips curve. Based on an open-economy New Keynesian framework applied to U.K. data, [Batini, Jackson, and Nickell \(2005\)](#) provide further evidence of the benefits of augmenting the Phillips curve with oil price to fit the data. Our approach captures the effects of oil prices not only on the conditional mean of inflation, but on the entire inflation distribution. Cross-quantile and cross-country variations in the parameters  $\gamma_\tau^i$  in Equation (2) capture its effects. Here again, we follow [Blanchard, Cerutti, and Summers \(2015\)](#) and impose  $\gamma_\tau^i \geq 0$ .<sup>6</sup>

The fourth risk factor  $f_t^i$  represents financial conditions. The literature has documented firms financing conditions also helps to explain inflation dynamics. Notable examples include [Del Negro, Giannoni, and Schorfheide \(2015\)](#), [Christiano, Eichenbaum, and Trabandt \(2015\)](#) and [Gilchrist et al. \(2017\)](#). More importantly, [López-Salido and Loria \(2022\)](#) extend the analysis to consider the effect of financial conditions on the inflation distribution, with a particular focus on downside risks to inflation. Following these authors, we approximate  $f_t^i$  by the Composite Indicator of Systemic Stress (CISS) developed by [Kremer, Lo Duca, and Holló \(2012\)](#), except for Luxembourg for which we use the Country-Level Index of Financial Stress (CLIFS) proposed by [Peltonen, Klaus, and Duprey \(2015\)](#). The CISS is a weekly index maintained by the ECB. It includes 15 raw series, mainly market-based financial stress measures that are split equally into five categories: financial intermediaries, money markets, equity markets, bond markets and foreign exchange markets. The CLIFS follows the approach of the CISS, but with slightly different market segments. The parameter associated with

---

<sup>5</sup>We also consider commodity and energy prices instead of oil price using the above-described specification of the augmented quantile Phillips curve. The results are robust to the choice of the series and are not reported here.

<sup>6</sup>[Blanchard, Cerutti, and Summers \(2015\)](#) consider import-price inflation in their estimated Phillips curve, that is proxied by oil price inflation at a monthly frequency in [López-Salido and Loria \(2022\)](#).

financial conditions in our empirical specification of the Phillips curve is  $\delta_\tau^i$ . This coefficient is left unconstrained in that case, since no consensus has been reached in the literature regarding the effect of financial conditions on the overall inflation distribution.

Finally, the last risk factor we consider is related to global supply chain pressures. Since the beginning of the COVID-19 pandemic, supply chain disruptions have become a major challenge for the global economy. Moreover, recent research by [Peersman \(2022\)](#) suggests that international food commodity prices explain a large part of variations in retail prices of food in the euro area through the food supply chain. We thus allow for supply chain conditions in Equation (2) to affect differently the conditional inflation quantiles. The variable  $sc_t$  is the global supply chain pressure index proposed by [Benigno et al. \(2022\)](#) and updated on a regular basis by the Federal Reserve Bank of New York. This series is built on variables that are meant to capture factors that put pressure on the global supply chain, both domestically and internationally. Its effects on the entire distribution of inflation is captured by the cross-quantile and cross-country parameters  $\phi_\tau^i$ . Following recent studies exploring the role of supply chain pressures in large post-COVID inflation fluctuations (see for instance [Amiti, Heise, and Wang, 2021](#) and [Di Giovanni et al., 2022](#)), we impose  $\phi_\tau^i \geq 0$ .

**II.2. The Conditional Inflation Distribution.** We generally report the direct estimates from the quantile regressions for the 10<sup>th</sup>, the 50<sup>th</sup>, and the 90<sup>th</sup> percentiles. We also map the quantile regression estimates into a skewed  $t$ -distribution along the lines of [Adrian, Boyarchenko, and Giannone \(2019\)](#) to recover and show a probability density function. The skewed  $t$ -distribution was developed by [Azzalini and Capitanio \(2003\)](#) and has the following form:

$$f(\bar{\pi}_{t+1,t+h}^i | x_t^i, \mu_t^i, \sigma_t^i, \eta_t^i, \kappa_t^i) = \frac{2}{\sigma_t^i} t(z_{t,t+h}^i; \kappa_t^i) T\left(\eta_t^i z_{t,t+h}^i \sqrt{\frac{\kappa_t^i + 1}{\kappa_t^i + (z_{t,t+h}^i)^2}}; \kappa_t^i + 1\right) \quad (3)$$

where  $z_{t,t+h}^i = \frac{\bar{\pi}_{t+1,t+h}^i(x_t) - \mu_t^i}{\sigma_t^i}$ , and  $t$  and  $T$  represent the density and cumulative distribution function of the student  $t$ -distribution, respectively. The four time-varying parameters of the distribution pin down the location  $\mu_t^i$ , scale  $\sigma_t^i$ , shape  $\eta_t^i$ , and fatness  $\kappa_t^i$  for each country  $i$ , where  $\eta_t^i$  and  $\kappa_t^i$  parameters control the skewness and the kurtosis of the distribution, respectively.

For each month and each country, we choose the four parameters  $(\mu_t, \sigma_t, \eta_t, \kappa_t)$  of the skewed  $t$ -distribution to minimize the squared distance between our estimated quantile function  $\hat{Q}_\tau(\bar{\pi}_{t+1,t+h}^i|x_t^i)$  obtained from the quantile Phillips curve model in Equation (2) and the quantile function of the skew  $t$ -distribution to match the 5<sup>th</sup>, 25<sup>th</sup>, 75<sup>th</sup> and 95<sup>th</sup> quantiles.

**II.3. Measuring Dispersion in Tail Risks.** Using our estimated predictive densities, we can construct informative measures of downside and upside risks. For each country, we define the concept of Inflation-at-Risk (IaR), the value at risk of future inflation. As made clear in López-Salido and Loria (2022), estimating the  $x^{th}$  quantile of the predictive inflation distribution is similar to constructing IaR measures at  $x\%$ . Hence, we refer to IaR to measure the probability that inflation falls below or above a given value in each country of our sample. IaR is defined by the quantiles of inflation rates for a given probability  $\alpha$  between periods  $t$  and  $t + h$  given  $x_t^i$  (the information set available at time  $t$  for country  $i$ ). To distinguish downside and upside risks, we define the downside IaR as

$$\Pr\left(\bar{\pi}_{t+1,t+h}^i \leq -IaR_{t+h}^i(\alpha|x_t^i)\right) = \alpha, \quad (4)$$

where  $-IaR_{t+h}^i(\alpha|x_t^i)$  is the downside IaR for country  $i$  in  $h$  months in the future at  $\alpha$  probability, typically equal to 10% in our empirical application. The upside IaR is defined as follows

$$\Pr\left(\bar{\pi}_{t+1,t+h}^i \geq +IaR_{t+h}^i(\alpha|x_t^i)\right) = \alpha, \quad (5)$$

where  $+IaR_{t+h}^i(\alpha|x_t^i)$  is the upside IaR for country  $i$  in  $h$  months in the future at  $\alpha$  probability.

Alternatively, we also rely on expected shortfall and longrise measures, which capture the severity of an event that occurs in either the left tail (for expected shortfall) or right tail (for expected longrise) of the predictive distribution. These two measures can be written as follows:

$$SF_{t+h}^i = \frac{1}{p} \int_0^p \hat{F}_{\bar{\pi}_{t+1,t+h}^i|x_t^i}^{-1}(\tau|x_t^i) d\tau, \quad LR_{t+h}^i = \frac{1}{p} \int_{1-p}^1 \hat{F}_{\bar{\pi}_{t+1,t+h}^i|x_t^i}^{-1}(\tau|x_t^i) d\tau, \quad (6)$$

for a chosen target probability  $p$ , and where  $\hat{F}^{-1}(\bullet)$  is the conditional inverse cumulative distribution of average future inflation over horizon  $h$  in country  $i$ . To be consistent with our choice for  $\alpha = 0.10$ , we set  $p = 0.10$  in our empirical application.

Once we have calculated risk measures, it is straightforward to obtain a measure of inflation dispersion across countries. Our preferred measure of dispersion is the cross-country standard

deviation of risks at horizon  $h$ , according to:

$$\sigma_{RISK_{t+h}^i} = \sqrt{\left[ \frac{1}{N} \sum_{i=1}^N (RISK_{t+h}^i - \overline{RISK}_{t+h})^2 \right]} \quad (7)$$

where  $RISK_{t+h}^i = [-IaR_{t+h}^i, +IaR_{t+h}^i, SF_{t+h}^i, LR_{t+h}^i]$ , and  $\overline{RISK}_{t+h}$  is the mean of our risk measures across countries.

### III. THE DISPERSION OF INFLATION-AT-RISK

This section describes the dispersion of inflation-at-risk for the euro area using the different metrics defined in Section II. Before focusing on the dispersion across countries, we discuss some results of Phillips curve estimates for each country of the sample.

**III.1. National Phillips Curve Estimates.** This section presents the results of the quantile Phillips curve estimates by country. The results are displayed in Tables B1 to B3 in Appendix B. Each table reports the estimated coefficients of the Equation (2) for each country for quantiles  $\tau = \{0.1, 0.5, 0.9\}$ , respectively. The last two rows of the tables report the unweighted means and the standard deviations of coefficients across countries.

First of all, the mean and the standard deviation of coefficient  $\lambda_\tau^i$  associated to long-term inflation expectations across countries remain stable over the quantiles. Overall, the weight of inflation expectations is greater than that of past inflation for all three quantiles. However, the anchoring is not the same when looking at the weight of inflation expectations country-by-country. For instance, the coefficient is equal to 1 in Germany in the middle or at the top of the distribution (50<sup>th</sup> and 90<sup>th</sup> quantiles), whereas it is equal to 0.56 at the bottom of the distribution (10<sup>th</sup> quantile). Inversely, the coefficient is equal to 1 in France at the bottom of the distribution but decreases to 0.69 and 0.74 in the middle and at the top of the distribution, respectively. Globally, inflation is weakly anchored in periphery countries (Italy, Spain, Ireland, Portugal and Greece), regardless of the quantile.

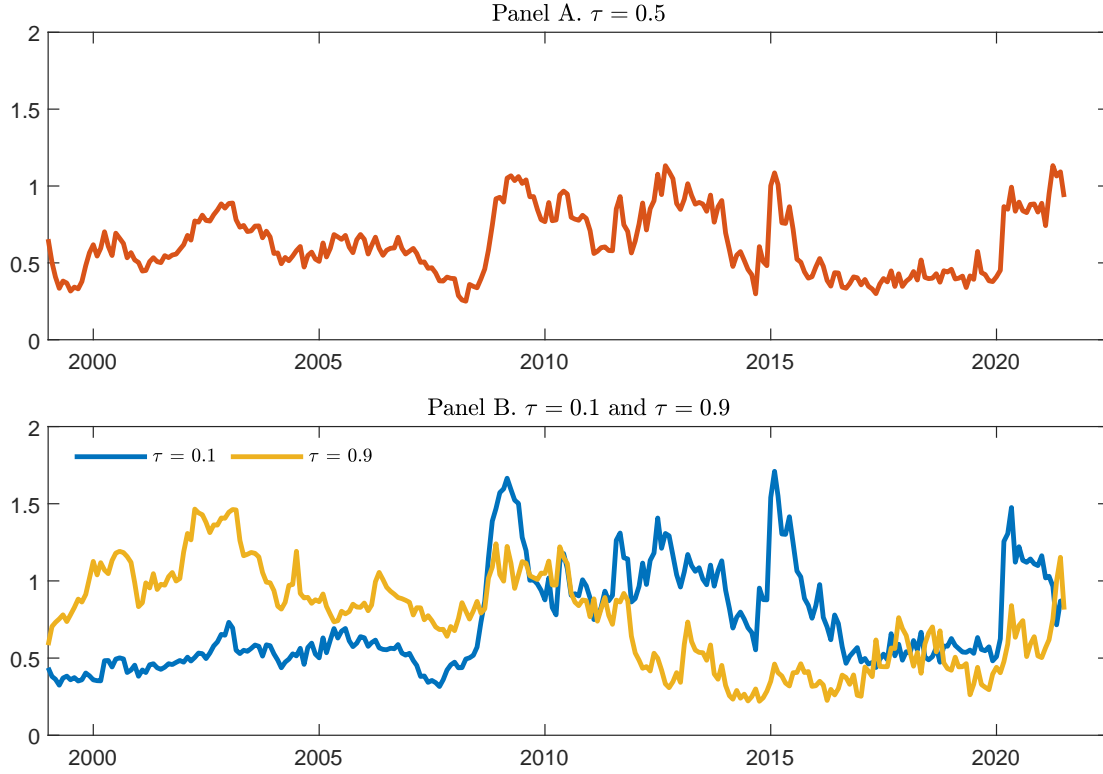
Focusing on the  $\theta_\tau^i$  coefficient (i.e. the slope of the Phillips curve), the magnitude of the cross-sectional mean is twice higher for the 50<sup>th</sup> and 90<sup>th</sup> quantiles than for the 10<sup>th</sup> quantile, though the coefficient is generally not significant from zero. Unemployment seems to affect inflation much more at the top of the distribution than at the bottom in the euro area, on average. This result suggests that labor market conditions matter more for upside risks to

inflation than for downside inflation risks. Such nonlinearities in the relationship between slack and inflation corroborate those from [Gagnon and Collins \(2019\)](#) in which the Phillips curve is normally steep but becomes nonlinear only when inflation is low. Once again, even if the cross-sectional standard deviation does not change significantly from a quantile to another, the estimated slope of the Phillips curve shows important disparities across countries within and between quantiles. For instance, the coefficient is strongly negative in the Netherlands for the 10<sup>th</sup> as for the 50<sup>th</sup> quantile, but is null at the top of the distribution. This highlights important disparities across countries for each quantile.

The cross-sectional mean of the coefficient associated with financial stress,  $\delta_{\tau}^i$ , is still negative with a magnitude almost seven times larger for the 10<sup>th</sup> quantile than in the 90<sup>th</sup> quantile (−1.29 against −0.19). This is consistent with the role of tighter financial conditions in the occurrence of low inflation episodes in the euro area. Our results corroborate a vast literature maintaining that there is a nonlinear relationship between financial sector and macroeconomy depending on the state of the economy. Notable examples include [He and Krishnamurthy \(2012, 2013\)](#) and [Brunnermeier and Sannikov \(2014\)](#) for the theory, and [Hubrich and Tetlow \(2015\)](#) and [Lhuissier \(2017\)](#) for the empirics. Since this coefficient is the only to be left unconstrained in the benchmark specification of the augmented Phillips curve model, it shows important disparities between euro area countries. The cross-sectional standard deviation is indeed very high for the three quantiles (1.33 for the 90<sup>th</sup> quantile, 1.63 for the 50<sup>th</sup> quantile, and 2.34 for the 10<sup>th</sup> quantile). However, as for the other estimated coefficients of the model, the effect of financial stress on inflation varies across countries and over the quantiles. For instance, the coefficient is positive at the top but negative at the bottom of the distribution in Austria (0.85 for the 90<sup>th</sup> quantile and −0.17 for the 10<sup>th</sup> quantile), whereas it is much higher (but always negative) in Greece at the bottom of the distribution (−5.84 for the 10<sup>th</sup> quantile, −5.48 for the 50<sup>th</sup> quantile, and −0.04 for the 90<sup>th</sup> quantile).

Capturing the effect of supply chain pressures on inflation, the  $\phi_{\tau}^i$  coefficient is similar from the 10<sup>th</sup> to the 50<sup>th</sup> quantile, but the mean and the standard deviation across countries is interestingly and considerably larger for at the top of the distribution. In line with the recent period, this suggests that tensions on global supply chain is a key feature of upside inflation risks across euro area countries.

FIGURE 2. Dispersion of conditional quantiles



*Note:* Standard deviation of conditional inflation quantiles  $\hat{Q}_\tau(\bar{\pi}_{t+1,t+h}^i | x_t^i)$  across country  $i$ , for quantiles  $\tau = \{0.1; 0.5; 0.9\}$  and forecast horizon  $h = 12$ . Panel A shows the standard deviation of the conditional quantile  $\tau = 0.5$ . Panel B shows the standard deviation of conditional quantiles  $\tau = 0.1$  and  $\tau = 0.9$ . Conditional quantiles  $\hat{Q}_\tau(\bar{\pi}_{t+1,t+h}^i | x_t^i)$  are simulated using the estimates of Equation (2). Figures D1 and D2 in Appendix D report the conditional quantiles by country.

Finally, the cross-sectional mean of the  $\gamma_\tau^i$  coefficient is slightly higher for the 90<sup>th</sup> quantile, suggesting that oil price affects upside risks to inflation more than downside inflation risks.

As a whole, and despite constrained coefficients (except on financial conditions), estimated national Phillips curve results show important non-linearities across quantiles. Moreover, it is worth noting that the non-linearities across quantiles are not the same for all countries, providing grounds for looking at the dispersion of conditional quantiles across euro area countries.

**III.2. Conditional Quantiles.** Figure 2 depicts the standard deviation of inflation quantiles across countries for the one-year forecast horizon. Panel A shows the evolution of the cross-sectional standard deviation of the 50<sup>th</sup> quantile over time, i.e. the median of the predictive

inflation distribution. The figure indicates no clear pattern of the dispersion of the 50<sup>th</sup> quantile over the entire sample period. Except for slight increases in troubled times — especially after the 2008 and the COVID crises, inflation dispersion in the middle of the distribution across countries displays a relatively stable evolution over time.

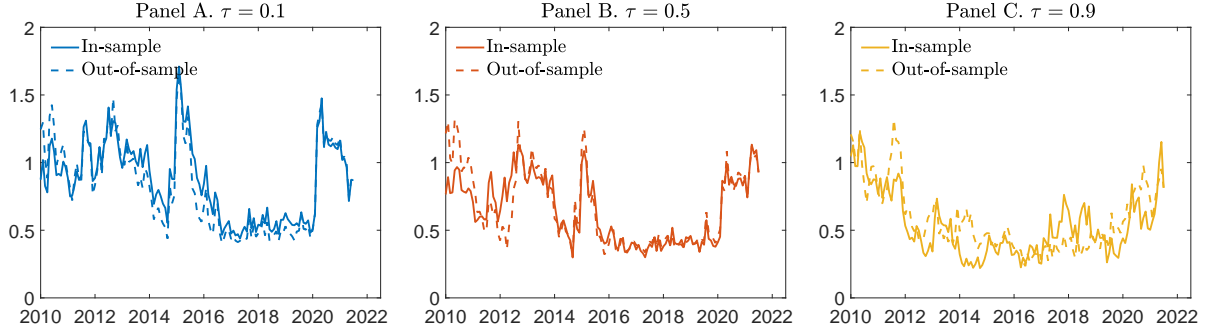
This is however not the case when looking at the tails of the dispersion of predictive inflation distribution across countries. Panel B plots the time-varying evolution of the standard deviation of the 10<sup>th</sup> and 90<sup>th</sup> quantiles of inflation distribution across countries. During the first decade of the euro area, inflation dispersion is clearly higher for the 90<sup>th</sup> quantile associated with risk of high inflation. Until 2005, the standard deviation of the 90<sup>th</sup> quantile is always higher than the standard deviations of the 10<sup>th</sup> quantile; its highest point is reached in 2003 during this period. Thereafter, until the Great Recession of 2008-2009, the inflation dispersion is low regardless of the quantile considered. These findings are consistent with the fact that the first decade of the euro area is still marked by the process of nominal convergence of countries that entered the euro area with different initial conditions in terms of inflation. In particular, some countries, such as Spain or Ireland, had inflation rates above the other countries.

From the Great Recession of 2008-09 to the COVID crisis, the situation is reversed. The highest inflation dispersions are for the 10<sup>th</sup> quantile associated with low inflation risk. The dispersion of the 90<sup>th</sup> quantile is overall lower than that of the 10<sup>th</sup> quantile, except in 2010 when all dispersion measures are high. The key highlight of this period is the spikes reached by the dispersion of the 10<sup>th</sup> quantile between 2008 and 2015. They exceed the dispersion levels observed during the first decade of the euro area. The succession of financial and sovereign debt crises during this period has clearly fueled the dispersion of inflation in the euro area through strong differentials in the risk of low inflation between these countries. In Appendix C, we illustrate this fact by comparing the full predictive inflation distribution of two polar economies of the euro area (Germany and Greece) before and during the financial crisis.

**III.3. Out-of-Sample Analysis.** In this section, we provide out-of-sample evidence of the results based on the quantile regression. Following [Adrian, Boyarchenko, and Giannone \(2019\)](#), we use data from January 1999 to December 2009, and we estimate the predictive distribution of inflation for December 2010 (one-year-ahead). Then, the procedure is repeated



FIGURE 3. Dispersion of conditional quantiles for out-of-sample forecasts



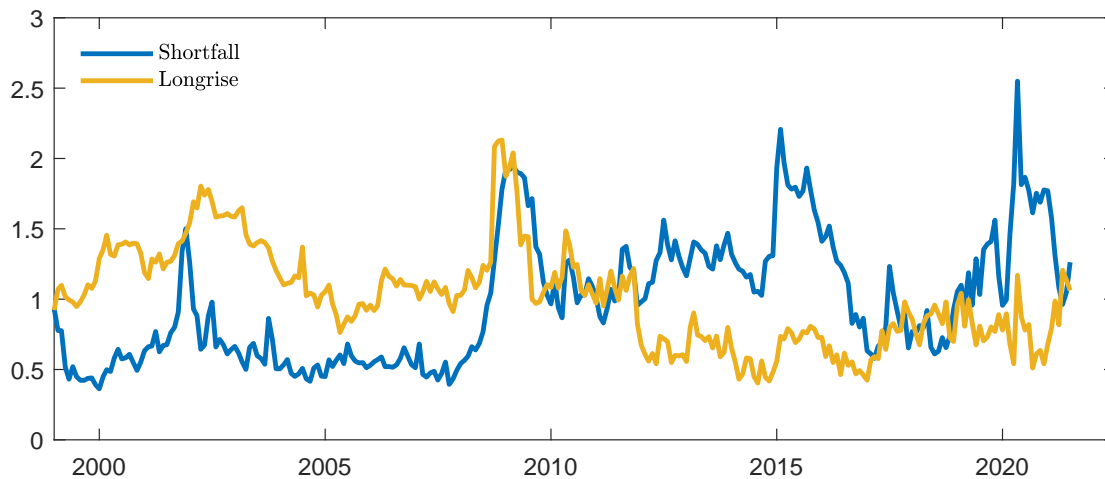
*Note:* Standard deviation of conditional inflation quantiles  $\hat{Q}_\tau(\bar{\pi}_{t+1,t+h}^i | x_t^i)$  across country  $i$ , for quantiles  $\tau = \{0.1; 0.5; 0.9\}$  and forecast horizon  $h = 12$ . Solid lines are for the in-sample estimates: conditional quantiles  $\hat{Q}_\tau(\bar{\pi}_{t+1,t+h}^i | x_t^i)$  are simulated using the estimates of Equation (2) using all the sample of data. Dotted lines are for the out-of-sample estimates: conditional quantiles  $\hat{Q}_\tau(\bar{\pi}_{t+1,t+h}^i | x_t^i)$  are simulated using a new estimate of Equation (2) for each new date  $t$  which is sequentially includes in the sample of data.

for each month until the end of the sample (i.e. July 2022). At each iteration, the sample is expanded through the estimation steps described earlier in Section II.

Results for the out-of-sample forecasting exercise are depicted in Figure 3. The figure shows that the in-sample and out-of-sample estimates of the quantiles are quite similar, except during the post-2010 euro area sovereign debt crisis regarding the 90<sup>th</sup> quantile (Panel C). Out-of-sample predictions also constantly overestimate the peak of the dispersion in the middle (50<sup>th</sup> quantile) and the bottom (10<sup>th</sup> quantile) of the distribution of inflation during the COVID crisis (Panels A and B). Otherwise, out-of-sample predictions for the selected quantiles of inflation dispersion are shown to perform well in tracking the evolution of the full sample estimation of this dispersion. Importantly, they exhibit good performance in predicting the recent increase in the dispersion of the risk of high inflation driven by spikes in 50<sup>th</sup> and 90<sup>th</sup> conditional quantiles (Panels B and C).

**III.4. Expected Shortfall and Longrise.** The dispersion of inflation quantiles is an interesting measure but it does not exploit all the information of the predictive inflation distribution. Indeed, as explained earlier, the  $x^{th}$  quantile gives the value of inflation such that there is  $x\%$  chance that inflation is below this value, but it does not depend on the exact distribution of inflation below this threshold. The interest of expected shortfall and longrise

FIGURE 4. Dispersion of inflation expected shortfall and longrise



*Note:* Standard deviation of expected shortfall and longrise  $SF_{t+h}^i$  and  $LR_{t+h}^i$  across country  $i$ , for  $p = 0.10$  and forecast horizon  $h = 12$ .  $SF_{t+h}^i$  and  $LR_{t+h}^i$  are defined by Equation (6). Figures D3 and D4 in Appendix D report the expected shortfall and longrise by country.

metrics developed by Adrian, Boyarchenko, and Giannone (2019) for economic growth is to exploit all this information. Following these authors, we apply these metrics to inflation differentials.

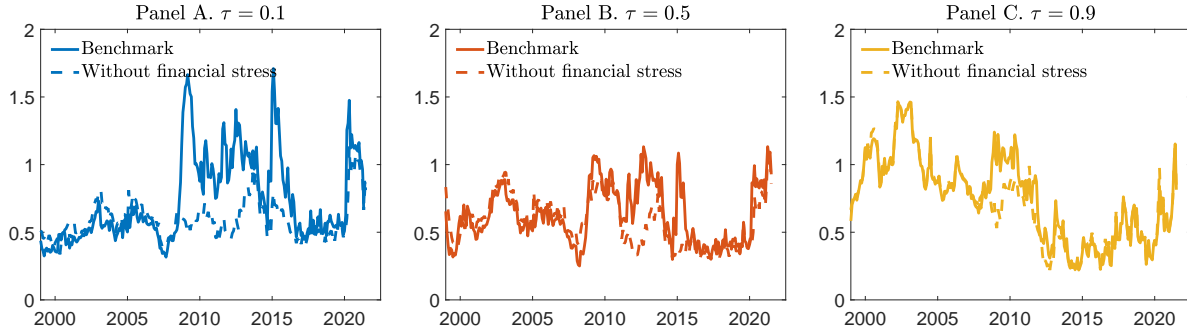
Figure 4 depicts the standard deviations of the longrises and shortfalls associated with the 10% risk level for the one-year ahead horizon. These figures confirm the pattern previously described using the dispersion of inflation quantiles. During the first decade of the euro area, the longrise outweighs the shortfall, while afterwards the shortfall is a more pronounced source of inflation dispersion.

#### IV. THE DRIVERS OF INFLATION DISPERSION

Having described the nature of the dispersion of the inflation in the euro area according to the nature of the extreme risk, either upside or downside, we investigate in this section the drivers of inflation dispersion. For this purpose, we elaborate counterfactual scenarios by muting selected explanatory variables in the right-hand side of the estimated quantile Phillips curve.

**IV.1. Financial Stress.** The first scenario assesses the role of financial conditions in the dynamics of inflation dispersion. We predict for each country the conditional quantiles of

FIGURE 5. Dispersion of conditional quantiles without financial stress



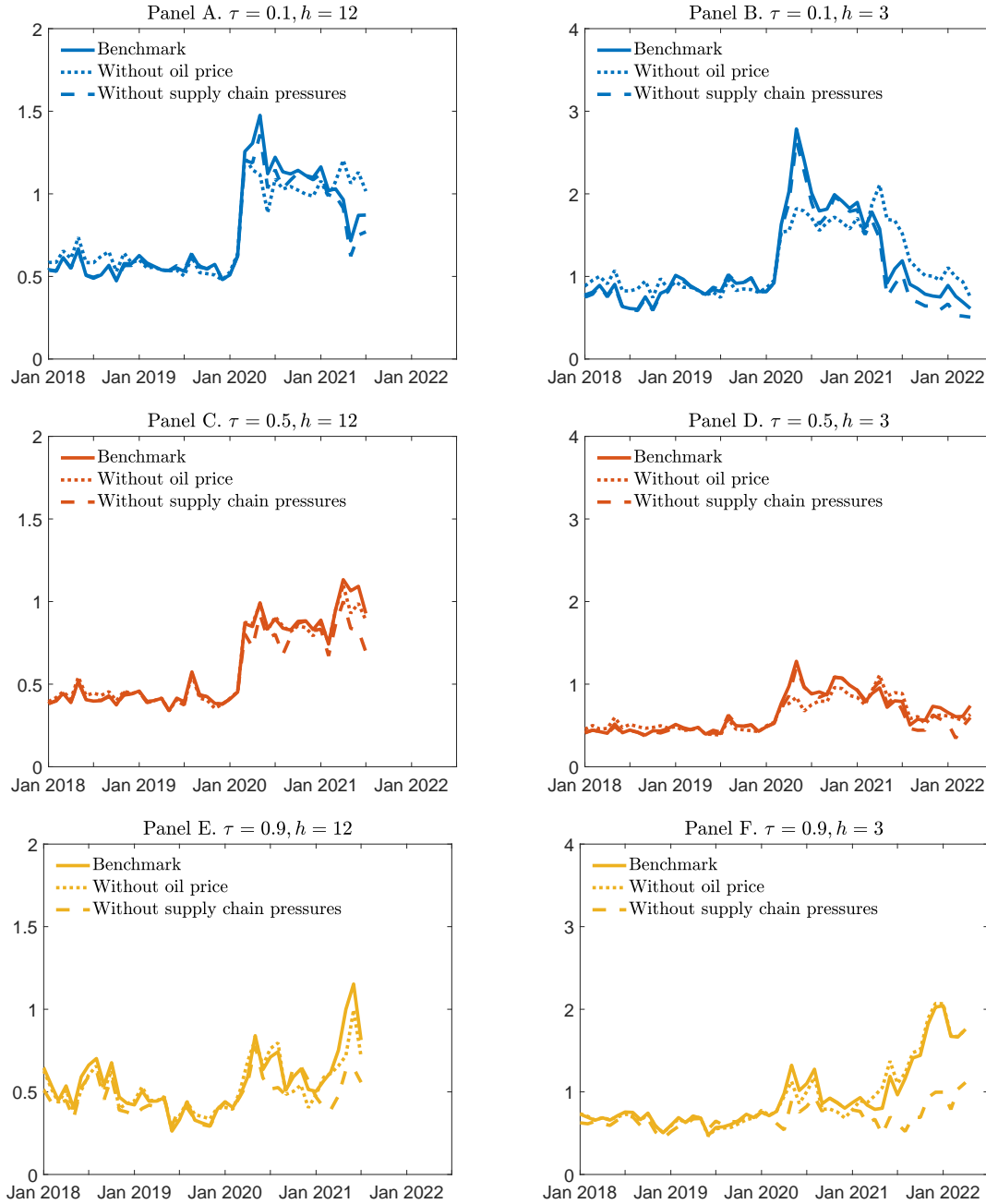
*Note:* The case without financial stress corresponds to the standard deviation of conditional quantiles predicted for  $f_t^i = 0$  in the quantile Phillips curve (2) for quantiles  $\tau = \{0.1; 0.5; 0.9\}$  and forecast horizon  $h = 12$ .

inflation under the assumption that the financial stress variable is set to zero for all countries at each date ( $f_t^i = 0$ ) in Equation (2). In this prediction, we keep the estimated values of the Phillips curve for each country and the realizations of the other economic variables unchanged. Figure 5 shows the results for the forecast horizon  $h = 12$ , and the three quantiles of interest,  $\tau = \{0.1, 0.5, 0.9\}$ . Each panel compares the benchmark inflation dispersion (solid lines) and the dispersion without financial stress (dashed lines).

Up to the Great Recession of 2008-2009, the euro area was immune to financial stress and therefore the predicted dispersion without this stress is very close to the benchmark. The role of financial stress then takes on great importance. This is especially the case for the 10<sup>th</sup> quantile. Looking at Panel A, the dispersion would have remained stable throughout the financial crisis period between 2008 and 2015 at a level three times smaller than the observed peaks. It is interesting to note that the absence of financial stress would also have led to less dispersion in inflation for the 50<sup>th</sup> quantile (Panel B). The results are however less striking for the 90<sup>th</sup> quantile, even if tighter financial conditions have still affected inflation dispersion.

These results are consistent with the common analysis of the role of financial crises in the extreme risk of deflation that weighed on the euro area. Since then, the situation has changed. International tensions in value chains and energy prices following the end of the COVID crisis and the war in Ukraine have raised the specter of a return to the extreme inflation of the 1970s.

FIGURE 6. Dispersion of conditional quantiles without oil price and supply chain pressures



*Note:* The case without oil price corresponds to the standard deviation of conditional quantiles predicted for  $\pi_t^{o,*} = \pi_t^{*,i}$  in the quantile Phillips curve (2). The case without supply chain pressures corresponds to the standard deviation of conditional quantiles predicted for  $sc_t = 0$  in the quantile Phillips curve (2). The first column of panels is for the one-year forecast ( $h = 12$ ) and the second one is for the one-quarter forecast ( $h = 3$ ). The first row of panels is for the 10<sup>th</sup> quantile, the second one for the 50<sup>th</sup> quantile, and the third one for the 90<sup>th</sup> quantile.

**IV.2. Pressures on Supply Chains and Energy Prices.** To analyze this recent period, we develop two scenarios: the scenario without oil price for  $\pi_t^{o,i} = \pi_t^{*,i}$  and the scenario without supply chain pressures for  $sc_t = 0$ . As before, for these predictions, we keep the estimated values of the Phillips curve for each country and the realizations of the other economic variables unchanged. Figure 6 shows the results for the three quantiles,  $\tau = \{0.1, 0.5, 0.9\}$  using core inflation. Each panel compares the benchmark inflation dispersion (solid lines), the dispersion without oil price (dotted lines), and the dispersion without supply chain pressures (dashed lines). We report results only for the period after 2018 to facilitate the interpretation of the figure.

The results are reported for two forecast horizons, one year and one quarter (i.e.  $h = 12$  and  $h = 3$ , respectively). The one-year forecast is more informative of trends than the one-quarter forecast. On the other hand, the advantage of the one-quarter forecast is that it provides information at a higher frequency. For instance, the abruptness of the COVID crisis is more accurately measured with the one-quarter forecast than with the one-year forecast, because inflation series are averaged over a shorter period. This explains why the peak observed in May 2020 greatly exceeds all other observed values of inflation dispersion for  $h = 3$ . The interest of the latter is also to be able to include in the analysis the last nine months of observation during the recent period marked by strong changes in the dynamics of inflation. More precisely, the one-quarter forecast has the ability to portray the dispersion of inflation until April 2022 (in the case where  $h = 3$ , the last point in April 2022 is the average of expected inflation between May and July 2022, given the data observed in April 2022), whereas the one-year forecast computes the dispersion of inflation based on data until July 2021 (recall that in the case where  $h = 12$ , the last point in July 2021 is the average of expected inflation between August 2021 and July 2022, given the data observed in July 2021). Therefore, looking at recent increase in oil price and supply chain pressures index over the last months (at least after July 2021), we expect that estimating the model with  $h = 3$  will allow to give new evidence on the effects of the recent evolution of oil price and supply chain pressures on the dispersion of inflation across euro area countries.<sup>7</sup>

---

<sup>7</sup>Estimates using  $h = 3$  take into account the peak observed in the [global supply chain pressures index](#) in December 2021, which is not covered when estimating the model using  $h = 12$ . Similarly, model estimates with  $h = 3$  include the recent and huge increase of more than 58% in the price of the barrel (in U.S. dollars) from December 2021 to March 2022, which is not covered when the model is estimated setting  $h = 12$ .

Supply chain tensions play a more prominent role than oil price in the dynamics of inflation dispersion. It is noteworthy that value chain pressures play a major role in the two extreme quantiles of inflation ( $10^{th}$  and  $90^{th}$ ). For both quantiles, inflation dispersion would have returned to pre-COVID values without the pressures on value chains.<sup>8</sup>

As a robustness check, we have also conducted those counterfactual exercises using HICP instead of core HICP. Considering headline inflation in the analysis confirm the previous results of the role of global supply chain in the evolution of inflation distribution. See Appendix E for further details.

**IV.3. Structural Heterogeneity.** We propose a last exercise of counterfactual scenarios to assess the role of economic structure heterogeneity in inflation dispersion. Inflation may diverge between countries, either because they are exposed to different economic events or because their different economic structures lead them to react differently to these events. To assess the respective role of structures and the economic context, we proceed as follows. We take France as a reference country. Then, we simulate the conditional quantiles of inflation under two assumptions: (i) all countries share the same Phillips curve coefficients as France, but are exposed to the economic variables actually observed in their own country; (ii) all countries are exposed to the same economic variables as France, but retain the estimated Phillips curve coefficients for each of them. Figure 7 shows the predicted inflation dispersion by quantiles under the two assumptions (we only consider in this case the one-year forecast). The dispersion of inflation is clearly higher when common economic series is considered (Panel A) than when we consider common structure (Panel B). This result indicates that the great heterogeneity in the national Phillips curves is the main driver of inflation dispersion in the euro area.

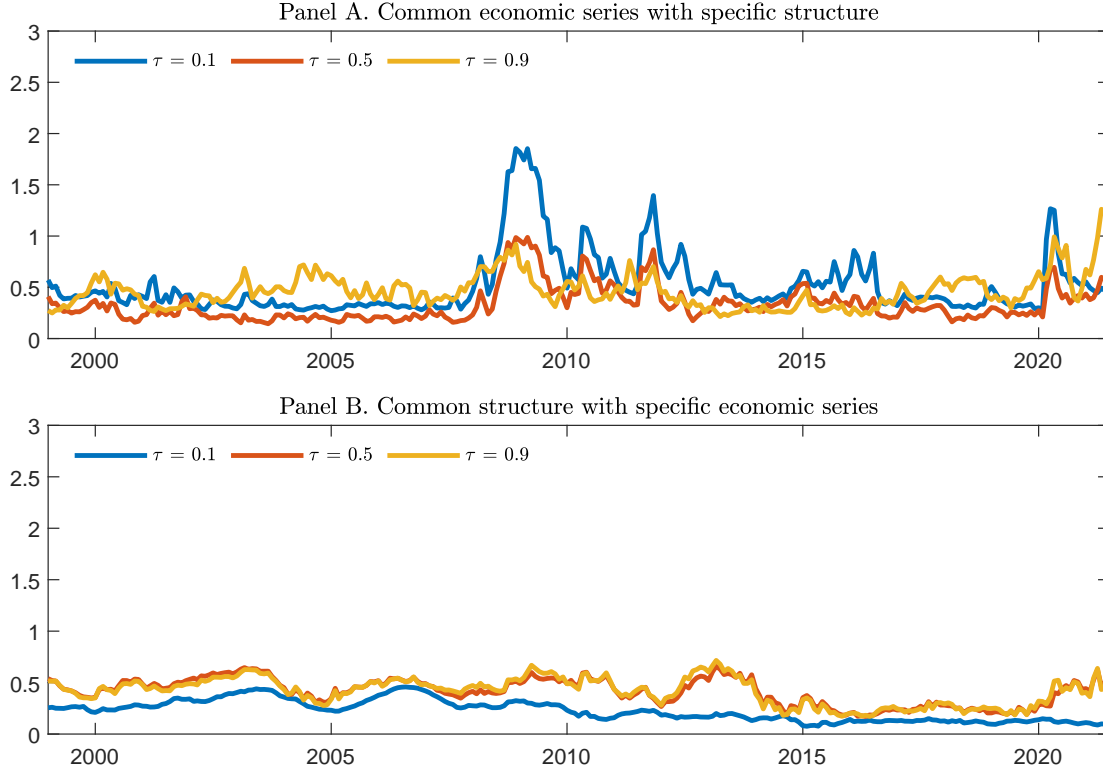
## V. ROBUSTNESS ANALYSIS: A MARKOV-SWITCHING APPROACH

In the existing literature, Markov-switching models have been proposed as an alternative method over quantile regressions to characterize business cycle variation in the probability

---

<sup>8</sup>To check the robustness of our results, we also run the benchmark model considering energy price rather than oil price. Despite differences in the two series over the last few months due to a record-high increase in natural gas prices in Europe, the results are robust to the choice of the series (the correlation between energy and oil prices is 0.96 from January 1999 to July 2022).

FIGURE 7. Dispersion of inflation quantiles for common structure or common economic series



*Note:* Standard deviation of conditional inflation quantiles  $\hat{Q}_\tau(\bar{\pi}_{t+1,t+h}^i | x_t^i)$  across country  $i$ , for quantiles  $\tau = \{0.1; 0.5; 0.9\}$  and forecast horizon  $h = 12$ . Panel A shows the standard deviation of the conditional quantiles assuming that all countries experienced the French economic series while preserving their own estimated coefficients for the Phillips curve. Panel B shows the standard deviation of the conditional quantiles assuming that all countries share the estimated coefficients for the French Phillips curve while preserving their own national economic series.

distribution and time-varying risks around GDP growth. Using a semi-structural model subject to Markov mean and variance shifts, [Caldara et al. \(2021\)](#) investigate the role of the financial and real conditions to predict tail risks in the U.S. economy. [Lhuissier \(2022\)](#) proposes a regime-switching skew-normal model to examine time variation in the third moment of the predictive distribution of euro area economic growth. [López-Salido and Loria \(2022\)](#) also propose a Markov-switching framework as an alternative method to study time variation in the predictive distribution of inflation in the U.S. This section follows this recent literature and adopts a Markov-switching framework as a robustness analysis.

**V.1. The Framework.** We employ a statistical model in which the observation  $\bar{\pi}_{t+1,t+h}^i$  is generated as follows:

$$\begin{aligned} \bar{\pi}_{t+1,t+h}^i = & \mu^i(s_t^i) + (1 - \lambda^i(s_t^i)) \pi_{t-1}^{*,i} + \lambda^i(s_t^i) \pi^{\text{LTE},i} + \theta^i(s_t^i) (u_t^i - u_t^{*,i}) + \\ & \gamma^i(s_t^i) (\pi_t^{o,*} - \pi_t^{*,i}) + \delta^i(s_t^i) f_t^i + \phi^i(s_t^i) sc_t + \sigma^i(s_t^i) \varepsilon_t^i, \end{aligned} \quad (8)$$

where  $\varepsilon_t^i$  follows a standard normal distribution, and  $s_t^i$  is an exogenous three-states first-order Markov process with the following transition matrix  $Q^i$

$$Q^i = \begin{bmatrix} q_{1,1}^i & q_{1,2}^i & q_{1,3}^i \\ q_{2,1}^i & q_{2,2}^i & q_{2,3}^i \\ q_{3,1}^i & q_{3,2}^i & q_{3,3}^i \end{bmatrix}, \quad (9)$$

where  $q_{u,v}^i = \Pr(s_t^i = u | s_{t-1}^i = v)$  denote the transition probabilities that  $s_t^i$  is equal to  $u$  given that  $s_{t-1}^i$  is equal to  $v$ , with  $u, v \in \{1, 2, 3\}$ ,  $q_{u,v}^i \geq 0$  and  $\sum_{v=1}^3 q_{u,v}^i = 1$ .

Our framework is subject to Markov mean and variance shifts over time. In particular, we impose three regimes of inflation, which can be considered as regimes of low (Regime 1), medium (Regime 2) and high (Regime 3) inflation. Both coefficients and standard deviations can change over time according to the same Markov process, meaning that the time of changes for coefficients is stochastically dependent of the times of changes for standard deviations.

We rely on Bayesian methods to estimate our Markov-switching model. When dealing with a Markov-switching model, the likelihood can be evaluated according to the [Hamilton \(1989\)](#)'s filter, and then combined with a prior distribution for the parameters. We use the idea of Gibbs sampling to obtain the empirical joint posterior density by sampling alternately from the following conditional posterior distribution. Our Gibbs sampler procedure begins with setting parameters at the peak of the posterior density function. The Monte Carlo Markov Chains (MCMC) sampling sequence involves a 4-block Gibbs sampler, in which we can generate in a flexible and straightforward manner alternatively draws from full conditional posterior distributions. Overall, our procedure follows the MCMC approach proposed by [Albert and Chib \(1993\)](#).

Regarding our prior, they are very dispersed and cover a large parameter space so that so that the data, through the likelihood, dominate the posterior distribution. It may be worth noting that we impose the exact same prior across regimes, so that the differences



in parameters between regimes result more from data (i.e., the likelihood) rather than priors. Moreover, we impose the same restrictions on the coefficients as those imposed in the estimation of quantile regressions.

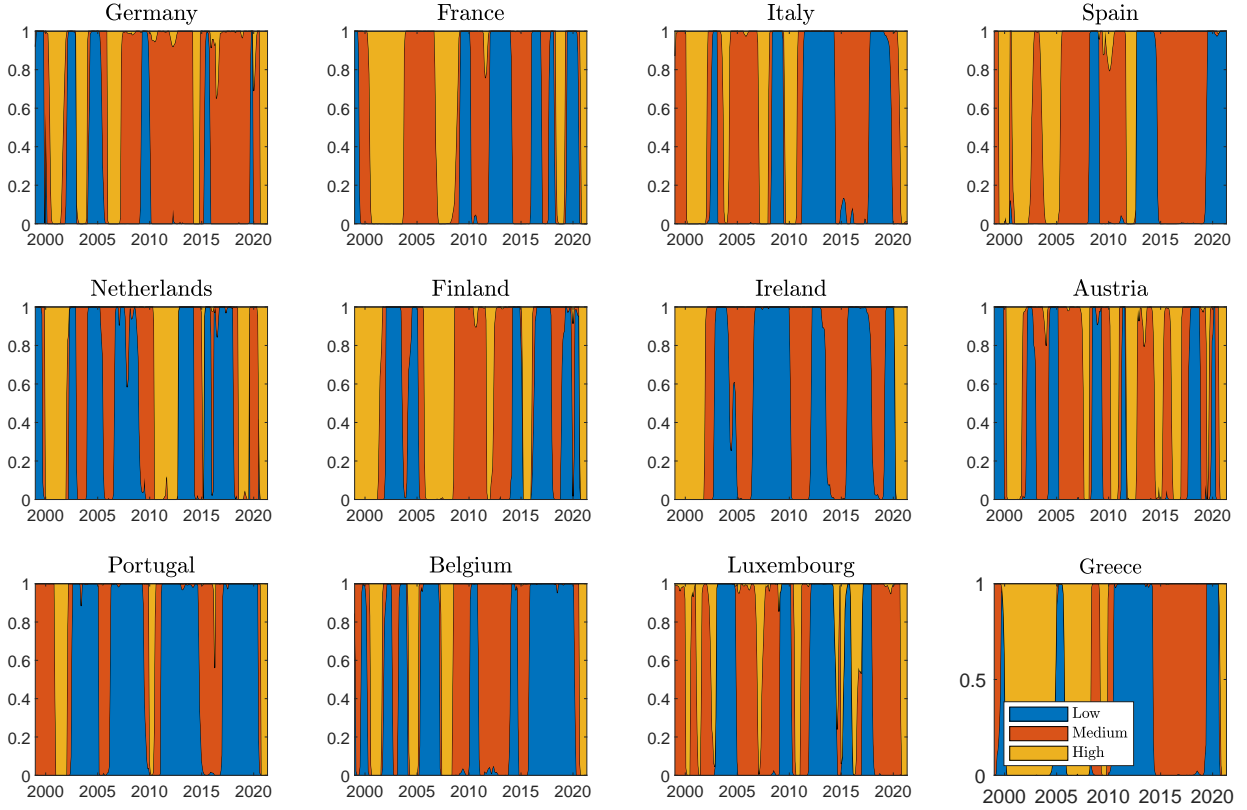
The online appendix provides the computational details for our maximization and MCMC procedures, as well as for the choice of the prior.

**V.2. Empirical Results.** Since we are studying whether a Markov-switching framework is able to produce quantitatively similar dispersion measures as those from a quantile regressions approach, we put in the appendix the estimates of Markov-switching Phillips curves by country — see Tables [F1](#), [F2](#), [F3](#) and [F4](#). However, it may worth saying that, in spite of differences in coefficients estimated at the country level, the results of cross-sectional mean and standard deviation give similar interpretation than those from the quantile regression model: high and stable anchoring of inflation expectations across inflation regimes (low, medium and high), steeper slope of the Phillips curve in medium and high than in low inflation regimes, key role of financial stress in low inflation regime with high dispersion across countries, and important role of global supply chain in high inflation regime.

Figure [8](#) reports the regime probabilities — evaluated at the mode — for each country. We report the smoothed probabilities in the sense of [Kim \(1994\)](#); i.e., full sample information is used in getting the regime probabilities at each date. One can see from the figure that each euro area country has been characterized by numerous switches between regimes over time. The times of changes are most of the time unsynchronized across countries, suggesting that the dispersion across countries is very much in evidence. For example, during the sovereign debt crisis in 2010-2012, countries most hit by the crisis like Portugal, Greece, Spain and Ireland, experienced a regime of low inflation, while others like Germany, Finland, and Austria were in a high or medium inflation regime. One exception regarding the divergence across countries is during the recent period where the high inflation regime has been the predominant regime for most of countries.

To provide a more formal analysis of the inflation dispersion and, to be more in line with the results of our quantile regressions, we also produce the cross-country dispersion of the expected shortfall and longrise measures produced from our Markov-switching model, as shown in Figure [9](#). Following [Lhuissier \(2022\)](#), the calculation of these measures follows a simulation procedure. First, we recover the smoothed regime probabilities for each date.

FIGURE 8. Regime Probabilities

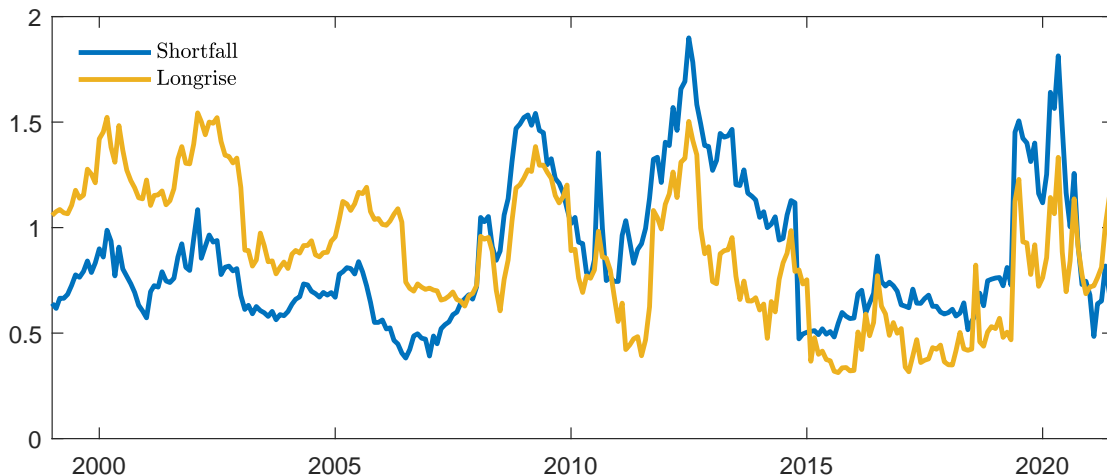


*Note:* Probabilities are smoothed in the sense of [Kim \(1994\)](#), i.e., full sample information is used in getting the regime probabilities at each date. The color code is as follows: blue (Regime 1, low inflation), red (Regime 2, medium inflation), yellow (Regime 3, high inflation).

Second, we generate our predictive distribution from the mixture of normal distributions using those probabilities as weights. Third, we compute the individual metrics using the empirical distribution, and then compute the dispersion measures. As shown by the figure, inflation dispersion is clearly higher for upside risks (expected longrise) than for downside risks (expected shortfall) during the first decade of the euro area. Thereafter, the pattern is reversed. The dispersion of downside risks prevails over upside risks since the Great Recession of 2008-2009. These findings are thus consistent with the stylized facts produced from quantile regressions as shown in [Figure 5](#).

Overall, our parametric Markov-switching framework is able to produce quantitatively similar results to the more flexible approach of Quantile Regressions of [Adrian, Boyarchenko,](#)

FIGURE 9. Dispersion of inflation expected shortfall and longrise from Markov-switching model



*Note:* Standard deviation of expected shortfall and longrise  $SF_{t+h}^i$  and  $LR_{t+h}^i$  across country  $i$  and for forecast horizon  $h = 12$ .  $SF_{t+h}^i$  and  $LR_{t+h}^i$  are computed using the Markov-switching model.

and Giannone (2019). We thus confirm the results of Caldara et al. (2021), that is, “the estimates of tail risk have robust features that can be captured with multiple models”.

## VI. CONCLUSION

To study inflation differentials in the euro area, we have adopted a “beyond the mean” approach by considering downside and upside inflation risks. This approach enabled us to identify three phases in the euro area. The first decade of the euro area where the risk of inflation dispersion in the euro area is associated with still significant upside risks despite the ongoing convergence process. The second decade of the euro area during which the risk of dispersion comes from downside risks to inflation or even deflation risks in a context of financial crises. The present period, in the wake of the COVID crisis with pressures on oil price and value chains, where the two risks, downside and upside, co-exist and feed the dispersion of inflation in the euro area.

Our results show that the high dispersion of extreme inflation risks described in this article is more the consequence of heterogeneous economic structures than of exposure to different national shocks. In this context, it is well known, at least since Benigno (2004), that targeting an average inflation rate of the monetary union, weighted by the size of the economies,

may not be optimal when union's members are heterogeneous. Instead, [Benigno \(2004\)](#) suggested targeting an average inflation rate using a weighting scheme that gives more weight to economies with the highest degree nominal rigidities—recently, [Kekre \(2022\)](#) proposes a similar analysis leading to giving greater weights to economies with more sclerotic labor markets. Future research would be of interest in investigating optimal monetary policy rules in the context of dispersed inflation tail risks.

## REFERENCES

- Adrian, T., N. Boyarchenko, and D. Giannone. 2019. "Vulnerable growth." *American Economic Review* 109:1263–89.
- Albert, J.H., and S. Chib. 1993. "Bayes Inference via Gibbs Sampling of Autoregressive Time Series Subject to Markov Mean and Variance Shifts." *Journal of Business & Economic Statistics* 11:1–15.
- Amiti, M., S. Heise, and A. Wang. 2021. "High Import Prices along the Global Supply Chain Feed Through to US Domestic Prices." Working paper, Federal Reserve Bank of New York.
- Andrade, P., V. Fourel, E. Ghysels, and J. Idier. 2014. "The financial content of inflation risks in the euro area." *International Journal of Forecasting* 30:648–659.
- Angeloni, I., and M. Ehrmann. 2007. "Euro area inflation differentials." *The BE Journal of Macroeconomics* 7.
- Azzalini, A., and A. Capitanio. 2003. "Distributions Generated by Perturbation of Symmetry with Emphasis on a Multivariate Skew t-distribution." *Journal of the Royal Statistical Society: Series B (Statistical Methodology)* 65:367–389.
- Ball, L., and S. Mazumder. 2021. "A Phillips curve for the euro area." *International Finance* 24:2–17.
- Banerjee, R.N., J. Contreras, A. Mehrotra, and F. Zampolli. 2020. "Inflation at risk in advanced and emerging market economies.", pp. .
- Batini, N., B. Jackson, and S. Nickell. 2005. "An open-economy new Keynesian Phillips curve for the UK." *Journal of Monetary Economics* 52:1061–1071.
- Beck, G.W., K. Hubrich, and M. Marcellino. 2009. "Regional inflation dynamics within and across euro area countries and a comparison with the United States." *Economic Policy* 24:142–184.

- Benigno, G., J. di Giovanni, J.J. Groen, and A.I. Noble. 2022. “A New Barometer of Global Supply Chain Pressures.” Liberty street economics, Federal Reserve Bank of New York.
- Benigno, P. 2004. “Optimal monetary policy in a currency area.” *Journal of international economics* 63:293–320.
- Blanchard, O., E. Cerutti, and L. Summers. 2015. “Inflation and Activity – Two Explorations and their Monetary Policy Implications.” Working Paper No. 21726, National Bureau of Economic Research, November.
- Botev, Z.I. 2017. “The normal law under linear restrictions: simulation and estimation via minimax tilting.” *Journal of the Royal Statistical Society Series B* 79:125–148.
- Brunnermeier, M.K., and Y. Sannikov. 2014. “A Macroeconomic Model with a Financial Sector.” *American Economic Review* 104:379–421.
- Caldara, D., D. Cascarini-Garcia, P. Cuba-Borda, and F. Loria. 2021. “Understanding Growth-at-Risk: A Markov-Switching Approach.” Unpublished.
- Carter, C.K., and R. Kohn. 1994. “On Gibbs Sampling for State Space Models.” *Biometrika* 81:541–553.
- Christiano, L.J., M.S. Eichenbaum, and M. Trabandt. 2015. “Understanding the Great Recession.” *American Economic Journal: Macroeconomics* 7:110–167.
- Cœuré, B. 2019. “Heterogeneity and the ECB’s monetary policy.” In *Speech at the Banque de France Symposium & 34th SUEF Colloquium on the occasion of the 20th anniversary of the euro on “The Euro Area: Staying the Course through Uncertainties”*, Paris. vol. 29.
- Coibion, O., and Y. Gorodnichenko. 2015. “Is the Phillips curve alive and well after all? Inflation expectations and the missing disinflation.” *American Economic Journal: Macroeconomics* 7:197–232.
- Coibion, O., Y. Gorodnichenko, and M. Ulate. 2019. “Is inflation just around the corner? The Phillips curve and global inflationary pressures.” In *AEA Papers and Proceedings*. vol. 109, pp. 465–69.
- Consolo, A., G. Koester, C. Nickel, M. Porqueddu, and F. Smets. 2021. “The need for an inflation buffer in the ECB’s price stability objective: The role of nominal rigidities and inflation differentials.” Working paper, ECB Occasional Paper.
- Del Negro, M., M.P. Giannoni, and F. Schorfheide. 2015. “Inflation in the Great Recession and New Keynesian Models.” *American Economic Journal: Macroeconomics* 7:168–196.

- Del Negro, M., M. Lenza, G.E. Primiceri, and A. Tambalotti. 2020. "What's Up with the Phillips Curve?" *Brookings Papers on Economic Activity*, pp. 301–358.
- Di Giovanni, J., S. Kalemli-Ozcan, A. Silva, and M.A. Yildirim. 2022. "Global Supply Chain Pressures, International Trade, and Inflation." Working paper, National Bureau of Economic Research.
- ECB. 2005. "Monetary policy and inflation differentials in a heterogeneous currency area." *Monthly Bulletin* 5:61–77.
- Eser, F., P. Karadi, P.R. Lane, L. Moretti, and C. Osbat. 2020. "The Phillips curve at the ECB." *The Manchester School* 88:50–85.
- Estrada, Á., J. Galí, and D. López-Salido. 2013. "Patterns of convergence and divergence in the euro area." *IMF Economic Review* 61:601–630.
- Figueres, J.M., and M. Jarociński. 2020. "Vulnerable growth in the euro area: Measuring the financial conditions." *Economics Letters* 191:109126.
- Gagnon, J.E., and C.G. Collins. 2019. "Low Inflation Bends the Phillips Curve." Working Paper Series No. WP19-6, Peterson Institute for International Economics, Apr.
- Geweke, J.F. 1996. *Bayesian Inference for Linear Models Subject to Linear Inequality Constraints*, New York, NY: Springer New York. pp. 248–263.
- Gilchrist, S., R. Schoenle, J. Sim, and E. Zakrajšek. 2017. "Inflation Dynamics during the Financial Crisis." *American Economic Review* 107:785–823.
- Haan, J.d. 2010. "Inflation differentials in the euro area: a survey." In *The European Central Bank at Ten*. Springer, pp. 11–32.
- Hamilton, J.D. 1989. "A New Approach to the Economic Analysis of Nonstationary Time Series and the Business Cycle." *Econometrica* 57:357–384.
- Hazell, J., J. Herreno, E. Nakamura, and J. Steinsson. 2022. "The slope of the Phillips Curve: evidence from US states." *The Quarterly Journal of Economics* 137:1299–1344.
- He, Z., and A. Krishnamurthy. 2013. "Intermediary Asset Prices." *American Economic Review* 103:1–43.
- . 2012. "A Model of Capital and Crises." *Review of Economic Studies* 79:735–777.
- Hubrich, K., and R.J. Tetlow. 2015. "Financial Stress and Economic Dynamics: The Transmission of Crises." *Journal of Monetary Economics* 70:100–115.

- Issing, O., I. Angeloni, V. Gaspar, H.J. Klöckers, K. Masuch, S. Nicoletti-Altimari, M. Ros-tagno, and F. Smets. 2003. “Background studies for the ECB’s evaluation of its monetary policy strategy.” *ECB*, pp. .
- Kekre, R. 2022. “Optimal currency areas with labor market frictions.” *American Economic Journal: Macroeconomics* 14:44–95.
- Kilian, L., and X. Zhou. 2021. “Oil prices, gasoline prices and inflation expectations.” *Journal of Applied Econometrics*, pp. .
- Kim, C.J. 1994. “Dynamic linear models with Markov-switching.” *Journal of Econometrics* 60:1–22.
- Koenker, R., and P. Ng. 2005. “Inequality Constrained Quantile Regression.” *Sankhyā: The Indian Journal of Statistics (2003-2007)* 67:418–440.
- Kremer, M., M. Lo Duca, and D. Holló. 2012. “CISS - a composite indicator of systemic stress in the financial system.” Working Paper Series No. 1426, European Central Bank, Mar.
- Lhuissier, S. 2022. “Financial Conditions and Macroeconomic Downside Risks in the Euro Area.” *European Economic Review* 143:1040–46.
- . 2017. “Financial Intermediaries’ Instability and Euro Area Macroeconomic Dynamics.” *European Economic Review* 98:49 – 72.
- López-Salido, J.D., and F. Loria. 2022. “Inflation at Risk.” Finance and Economics Discussion Series No. 2020-013, Board of Governors of the Federal Reserve System (U.S.), Feb.
- Matheson, T., and E. Stavrev. 2013. “The Great Recession and the inflation puzzle.” *Economics Letters* 120:468–472.
- Peersman, G. 2022. “International Food Commodity Prices and Missing (Dis)Inflation in the Euro Area.” *The Review of Economics and Statistics* 104:85–100.
- Peltonen, T.A., B. Klaus, and T. Duprey. 2015. “Dating systemic financial stress episodes in the EU countries.” Working Paper Series No. 1873, European Central Bank, Dec.
- Plagborg-Møller, M., L. Reichlin, G. Ricco, and T. Hasenzagl. 2020. “When is growth at risk?” *Brookings Papers on Economic Activity* 2020:167–229.
- Reichlin, L., K. Adam, W.J. McKibbin, M. McMahon, R. Reis, G. Ricco, and B. Weder di Mauro. 2021. *The ECB strategy: The 2021 review and its future*. Centre for Economic Policy Research.

- Salisu, A.A., I. Ademuyiwa, and K.O. Isah. 2018. "Revisiting the forecasting accuracy of Phillips curve: the role of oil price." *Energy Economics* 70:334–356.
- Sims, C.A., D.F. Waggoner, and T. Zha. 2008. "Methods for Inference in Large Multiple-equation Markov-switching Models." *Journal of Econometrics* 146:255–274.



# ONLINE APPENDIX: THE RISK OF INFLATION DISPERSION IN THE EURO AREA

STÉPHANE LHUISSIER, AYMERIC ORTMANS AND FABIEN TRIPIER

This Appendix consists of the following sections:

- A. Data
- B. National Phillips Curve Estimates (tables)
- C. Case Study: Germany and Greece During the Financial Crisis
- D. Expected Shortfall and Longrise by Country
- E. Counterfactual exercises using HICP
- F. Markov-switching Procedure
  - F.1. The Posterior Density
  - F.2. Additional Results

## APPENDIX A. DATA

All variables are monthly time series covering January 1999 through July 2022. The following variables use data obtained directly from different sources:

- Harmonized Index of Consumer Prices
  - Source: ECB - ICP (Indices of Consumer prices)
  - Details: Monthly – Neither seasonally nor working day adjusted – HICP - All-items excluding energy and food – Eurostat – Index
  - Data transformation: Authors’ calculations using the x13 toolbox to get seasonally adjusted series for each euro area member countries.
- Unemployment rate
  - Source: Eurostat - Unemployment by sex and age – monthly data
  - Details: Monthly – Seasonally adjusted data, not calendar adjusted data – Total – Percentage of population in the labor force
- Natural Rate of Unemployment
  - Source: Authors’ calculations
  - Details: HP-filtered trend (with smoothing parameter  $\lambda = 14,400$  of unemployment rate).
- Oil Prices
  - Source: U.S. Energy Information Administration - Spot Prices
  - Details: Crude Oil Prices: Brent - Europe - Dollars per Barrel, Not Seasonally Adjusted
- Supply Chain index
  - Source: New York Fed’s [website](#)
  - Details: Global Supply Chain Pressure Index (GSCPI)
- Financial conditions (CISS)
  - Source: ECB - CISS
  - Details: Daily – ECB – Economic indicator – New Composite Indicator of Systemic Stress (CISS) – Index
  - Data transformation: Authors’ calculations to get monthly average of the series.
- Financial conditions (CLIFS)
  - Source: ECB - CLIFS

- Details: Monthly – ECB – Economic indicator – Country-Level Index of Financial Stress (CLIFS) Composite Indicator – Index
- Long-Term Inflation Expectations
  - Source: Consensus Economics
  - Details: Six-to-ten-year-ahead mean CPI inflation forecasts.
  - Data transformation: Euro area forecasts for Luxembourg (no forecast available), spline interpolation for all missing data in April 1999.

# APPENDIX B. NATIONAL PHILLIPS CURVE ESTIMATES (TABLES)

TABLE B1. Phillips curve estimates for the 10<sup>th</sup> quantile

	$\hat{\mu}_\tau^i$	$\hat{\lambda}_\tau^i$	$\hat{\theta}_\tau^i$	$\hat{\gamma}_\tau^i$	$\hat{\delta}_\tau^i$	$\hat{\phi}_\tau^i$
Germany	-1.07 [-1.20;-0.94]	0.56 [0.30;0.81]	-0.00 [-0.14;0.14]	0.41 [0.21;0.61]	0.78 [0.35;1.20]	0.13 [0.01;0.25]
France	-1.15 [-1.38;-0.93]	1.00 [0.79;1.21]	-0.00 [-0.17;0.17]	0.26 [0.02;0.51]	-0.84 [-1.51;-0.17]	0.13 [0.04;0.22]
Italy	-0.60 [-0.72;-0.48]	0.20 [0.09;0.31]	-0.00 [-0.11;0.11]	-0.00 [-0.07;0.07]	-1.34 [-1.95;-0.73]	0.00 [-0.05;0.05]
Spain	-0.89 [-1.31;-0.47]	0.52 [0.24;0.79]	-0.00 [-0.15;0.15]	0.38 [-0.12;0.87]	-4.20 [-5.85;-2.54]	0.13 [-0.01;0.27]
Netherlands	-1.16 [-1.25;-1.08]	0.88 [0.80;0.95]	-0.78 [-0.97;-0.58]	0.37 [0.19;0.56]	0.35 [-0.13;0.83]	0.22 [0.13;0.30]
Finland	-0.97 [-1.11;-0.83]	0.38 [0.22;0.53]	-0.08 [-0.20;0.03]	0.18 [-0.13;0.49]	1.00 [0.36;1.65]	0.33 [0.21;0.45]
Ireland	-1.37 [-1.63;-1.10]	0.81 [0.60;1.02]	-0.00 [-0.05;0.05]	0.39 [-0.17;0.94]	-4.85 [-6.85;-2.84]	0.06 [-0.11;0.22]
Austria	-0.58 [-0.68;-0.47]	0.76 [0.63;0.89]	-0.00 [-0.05;0.05]	-0.00 [-0.05;0.05]	-0.17 [-0.58;0.23]	0.13 [0.06;0.20]
Portugal	-1.24 [-1.45;-1.02]	0.51 [0.38;0.63]	-0.00 [-0.05;0.05]	0.40 [0.03;0.76]	-0.66 [-1.43;0.11]	0.00 [-0.01;0.01]
Belgium	-0.63 [-0.67;-0.60]	1.00 [0.97;1.03]	-0.00 [-0.08;0.08]	0.02 [-0.03;0.06]	0.30 [0.06;0.54]	0.03 [-0.01;0.06]
Luxembourg	-0.54 [-0.67;-0.41]	0.82 [0.61;1.03]	-0.00 [-0.14;0.14]	0.52 [0.31;0.74]	0.02 [-0.71;0.75]	0.11 [0.02;0.21]
Greece	-0.96 [-1.69;-0.22]	0.43 [0.29;0.58]	-0.14 [-0.33;0.06]	1.42 [0.22;2.61]	-5.84 [-7.73;-3.95]	0.00 [-0.11;0.11]
Mean	-0.93	0.65	-0.08	0.36	-1.29	0.11
Std. Dev.	0.28	0.26	0.22	0.38	2.34	0.10

Note: Table B1 displays the coefficients of the quantile Phillips curve defined by Equation (2):

$$\hat{Q}_\tau(\bar{\pi}_{t+1,t+h}^i|x_t^i) = \hat{\mu}_\tau^i + \left(1 - \hat{\lambda}_\tau^i\right) \pi_{t-1}^{*,i} + \hat{\lambda}_\tau^i \pi^{\text{LTE},i} + \hat{\theta}_\tau^i \left(u_t^i - u_t^{*,i}\right) + \hat{\gamma}_\tau^i \left(\pi_t^{o,*} - \pi_t^{*,i}\right) + \hat{\delta}_\tau^i f_t^i + \hat{\phi}_\tau^i sc_t$$

estimated by country for the 10<sup>th</sup> quantile. The last two rows show the unweighted means and the standard deviations of coefficients across countries.

TABLE B2. Phillips curve estimates for the 50<sup>th</sup> quantile

	$\hat{\mu}_\tau^i$	$\hat{\lambda}_\tau^i$	$\hat{\theta}_\tau^i$	$\hat{\gamma}_\tau^i$	$\hat{\delta}_\tau^i$	$\hat{\phi}_\tau^i$
Germany	-0.47 [-0.55;-0.38]	1.00 [0.95;1.05]	-0.27 [-0.44;-0.10]	0.16 [0.05;0.27]	-0.33 [-0.59;-0.07]	0.25 [0.15;0.35]
France	-0.20 [-0.36;-0.03]	0.69 [0.54;0.84]	-0.25 [-0.46;-0.05]	0.33 [0.17;0.49]	-1.46 [-2.03;-0.89]	0.00 [-0.08;0.08]
Italy	0.07 [-0.05;0.19]	0.24 [0.12;0.36]	-0.03 [-0.24;0.18]	-0.00 [-0.11;0.11]	-1.57 [-2.26;-0.88]	0.04 [-0.06;0.14]
Spain	-0.15 [-0.25;-0.05]	0.47 [0.35;0.60]	-0.00 [-0.06;0.06]	0.25 [0.02;0.47]	-1.10 [-2.12;-0.08]	0.00 [-0.04;0.04]
Netherlands	-0.38 [-0.56;-0.20]	0.71 [0.56;0.85]	-0.67 [-0.98;-0.35]	0.58 [0.34;0.82]	0.25 [-0.92;1.42]	0.30 [0.12;0.48]
Finland	-0.11 [-0.22;0.00]	0.19 [0.06;0.32]	-0.00 [-0.06;0.06]	0.55 [0.21;0.90]	0.50 [-0.30;1.30]	0.34 [0.23;0.45]
Ireland	-0.22 [-0.45;0.01]	0.46 [0.29;0.63]	-0.00 [-0.13;0.13]	1.12 [0.58;1.67]	-2.05 [-4.11;0.00]	0.27 [0.07;0.46]
Austria	-0.07 [-0.15;0.00]	0.99 [0.93;1.05]	-0.00 [-0.05;0.05]	0.17 [0.05;0.29]	-0.05 [-0.70;0.60]	0.24 [0.13;0.34]
Portugal	-0.21 [-0.41;-0.01]	0.47 [0.30;0.64]	-0.00 [-0.14;0.14]	0.31 [-0.07;0.69]	-1.51 [-2.72;-0.30]	0.00 [-0.09;0.09]
Belgium	-0.28 [-0.37;-0.18]	1.00 [0.96;1.04]	-0.08 [-0.21;0.05]	-0.00 [-0.06;0.06]	0.22 [-0.19;0.62]	0.04 [-0.01;0.09]
Luxembourg	-0.02 [-0.13;0.09]	0.81 [0.67;0.95]	-0.24 [-0.40;-0.08]	0.50 [0.35;0.64]	-0.28 [-0.87;0.32]	0.08 [-0.01;0.17]
Greece	0.34 [0.07;0.61]	0.46 [0.37;0.55]	-0.36 [-0.62;-0.10]	0.09 [-0.32;0.50]	-5.48 [-7.96;-3.00]	0.00 [-0.10;0.10]
Mean	-0.14	0.62	-0.16	0.34	-1.07	0.13
Std. Dev.	0.21	0.29	0.21	0.32	1.63	0.14

Note: Table B2 displays the coefficients of the quantile Phillips curve defined by Equation (2):

$$\hat{Q}_\tau(\bar{\pi}_{t+1,t+h}^i|x_t^i) = \hat{\mu}_\tau^i + (1 - \hat{\lambda}_\tau^i) \pi_{t-1}^{*,i} + \hat{\lambda}_\tau^i \pi^{\text{LTE},i} + \hat{\theta}_\tau^i (u_t^i - u_t^{*,i}) + \hat{\gamma}_\tau^i (\pi_t^{o,*} - \pi_t^{*,i}) + \hat{\delta}_\tau^i f_t^i + \hat{\phi}_\tau^i sc_t$$

estimated by country for the 50<sup>th</sup> quantile. The last two rows show the unweighted means and the standard deviations of coefficients across countries.

TABLE B3. Phillips curve estimates for the 90<sup>th</sup> quantile

	$\hat{\mu}_\tau^i$	$\hat{\lambda}_\tau^i$	$\hat{\theta}_\tau^i$	$\hat{\gamma}_\tau^i$	$\hat{\delta}_\tau^i$	$\hat{\phi}_\tau^i$
Germany	0.43 [0.27;0.58]	1.00 [0.97;1.03]	-0.00 [-0.06;0.06]	0.00 [-0.13;0.13]	-1.14 [-1.56;-0.73]	0.42 [0.22;0.62]
France	0.37 [0.25;0.48]	0.74 [0.64;0.84]	-0.42 [-0.61;-0.23]	0.03 [-0.07;0.12]	-1.71 [-2.09;-1.33]	0.28 [0.15;0.42]
Italy	0.80 [0.64;0.97]	0.43 [0.20;0.66]	-0.22 [-0.49;0.06]	-0.00 [-0.24;0.24]	0.71 [-0.82;2.24]	0.00 [-0.11;0.11]
Spain	0.75 [0.46;1.04]	0.63 [0.44;0.82]	-0.00 [-0.24;0.24]	0.60 [0.25;0.95]	-1.02 [-2.31;0.27]	0.18 [0.00;0.36]
Netherlands	0.58 [0.19;0.97]	0.42 [0.19;0.64]	-0.00 [-0.66;0.66]	1.35 [0.77;1.92]	2.48 [-0.61;5.58]	0.16 [-0.02;0.35]
Finland	0.46 [0.29;0.62]	0.55 [0.39;0.71]	0.00 [-0.04;0.04]	0.85 [0.67;1.02]	1.33 [0.06;2.61]	0.32 [0.21;0.44]
Ireland	1.80 [1.33;2.28]	0.14 [-0.04;0.33]	-0.00 [-0.25;0.25]	1.21 [0.62;1.80]	-1.67 [-4.04;0.71]	0.82 [0.50;1.14]
Austria	0.54 [0.38;0.71]	1.00 [0.93;1.07]	-0.00 [-0.07;0.07]	0.47 [0.24;0.70]	0.85 [0.06;1.63]	0.53 [0.33;0.73]
Portugal	1.92 [1.36;2.47]	0.19 [-0.02;0.40]	-0.34 [-0.65;-0.03]	1.00 [0.54;1.46]	-1.65 [-3.98;0.68]	0.86 [0.51;1.21]
Belgium	0.71 [0.54;0.89]	1.00 [0.99;1.01]	-0.69 [-0.91;-0.47]	0.27 [0.06;0.49]	-0.22 [-0.85;0.40]	0.39 [0.21;0.56]
Luxembourg	0.52 [0.38;0.66]	0.75 [0.63;0.87]	-0.00 [-0.16;0.16]	0.48 [0.33;0.64]	-0.16 [-0.73;0.41]	0.32 [0.20;0.45]
Greece	1.14 [0.80;1.48]	0.63 [0.47;0.80]	-0.01 [-0.24;0.21]	1.22 [0.77;1.67]	-0.04 [-2.19;2.11]	0.26 [-0.03;0.56]
Mean	0.83	0.62	-0.14	0.62	-0.19	0.38
Std. Dev.	0.52	0.30	0.23	0.50	1.33	0.25

Note: Table B3 displays the coefficients of the quantile Phillips curve defined by Equation (2):

$$\hat{Q}_\tau(\pi_{t+1,t+h}^i|x_t^i) = \hat{\mu}_\tau^i + (1 - \hat{\lambda}_\tau^i)\pi_{t-1}^{*,i} + \hat{\lambda}_\tau^i\pi_{t-1}^{\text{LTE},i} + \hat{\theta}_\tau^i(u_t^i - u_t^{*,i}) + \hat{\gamma}_\tau^i(\pi_t^{o,*} - \pi_t^{*,i}) + \hat{\delta}_\tau^i f_t^i + \hat{\phi}_\tau^i sc_t$$

estimated by country for the 90<sup>th</sup> quantile. The last two rows show the unweighted means and the standard deviations of coefficients across countries.

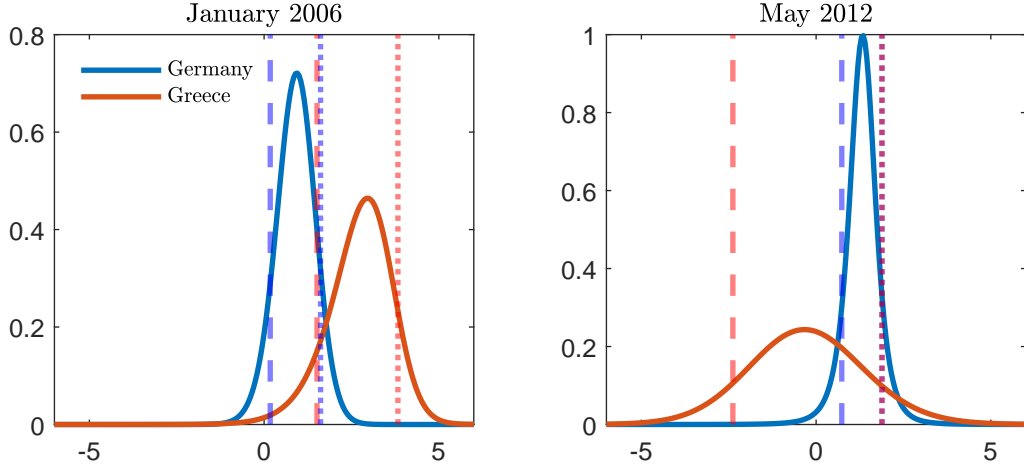
## APPENDIX C. CASE STUDY: GERMANY AND GREECE DURING THE FINANCIAL CRISIS

In this section, we propose a case study to illustrate the situation of increasing dispersion of downside inflation risks. We compare the conditional distributions of predicted inflation for two polar countries of the euro area, Germany and Greece, for two specific dates. The first one, January 2006, reflects the quiet period of the euro area. The second, May 2012, is instead in the period of financial turmoil. Figure C1 shows the conditional distribution of inflation forecast one year ahead ( $h = 12$ ) using the estimated skewed  $t$ -density functions defined by Equation (3) for each country at these two dates.

In January 2006, predicted inflation is higher in Greece than in Germany. The distribution for Greece is shifted to the right compared to Germany. For this date, the dispersion is homogeneous for the whole distribution (the differences between the quantiles are between 1.34 and 2.21 percentage points of inflation).

The situation is radically different in May 2012, mainly due to the change in the distribution of inflation in Greece. Greece is then subject to a severe risk of deflation. The distribution of inflation has shifted to the left but it has also flattened considerably giving rise to a high level of downside inflation risk. There is then a 10% chance that inflation will be below -2.38% in the coming year. In terms of dispersion, this is no longer homogeneous for the entire distribution in May 2012, unlike January 2006. The 10<sup>th</sup> quantile for Greece is 3.17 percentage points lower than that of Germany. This is almost twice as much as the gap in the 50<sup>th</sup>. Interestingly, the gap in the 90<sup>th</sup> quantile is now very close to zero, meaning that the dispersion of inflation rates between Germany and Greece in May 2012 has not been associated with the dispersion of quantiles at the top of the distribution. May 2012 is thus a typical example of high risk of inflation dispersion from the bottom of the distribution, i.e. associated with an extreme risk of low inflation.

FIGURE C1. Probability densities

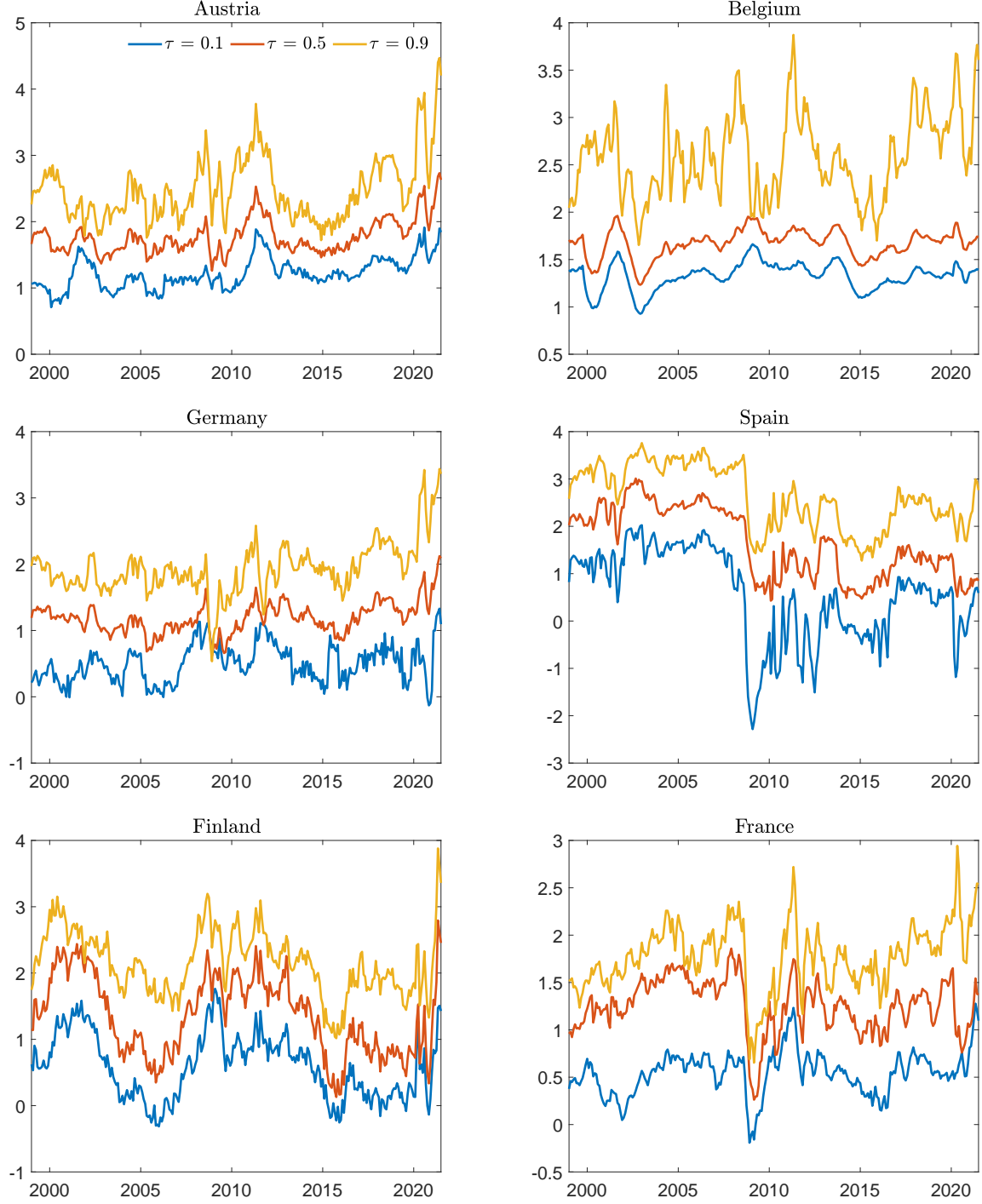


*Note:* Estimated skewed  $t$ -density functions defined by Equation (3) for one-year-ahead ( $h = 12$ ) inflation rates for Germany and Greece in January 2006 (left panel) and May 2012 (right panel). Vertical lines represent the respective quantiles extracted from the estimated distribution: dashed blue (red) lines represent quantile  $\tau = 0.1$  for Germany (Greece), and dotted blue (red) lines represent quantile  $\tau = 0.9$  for Germany (Greece).



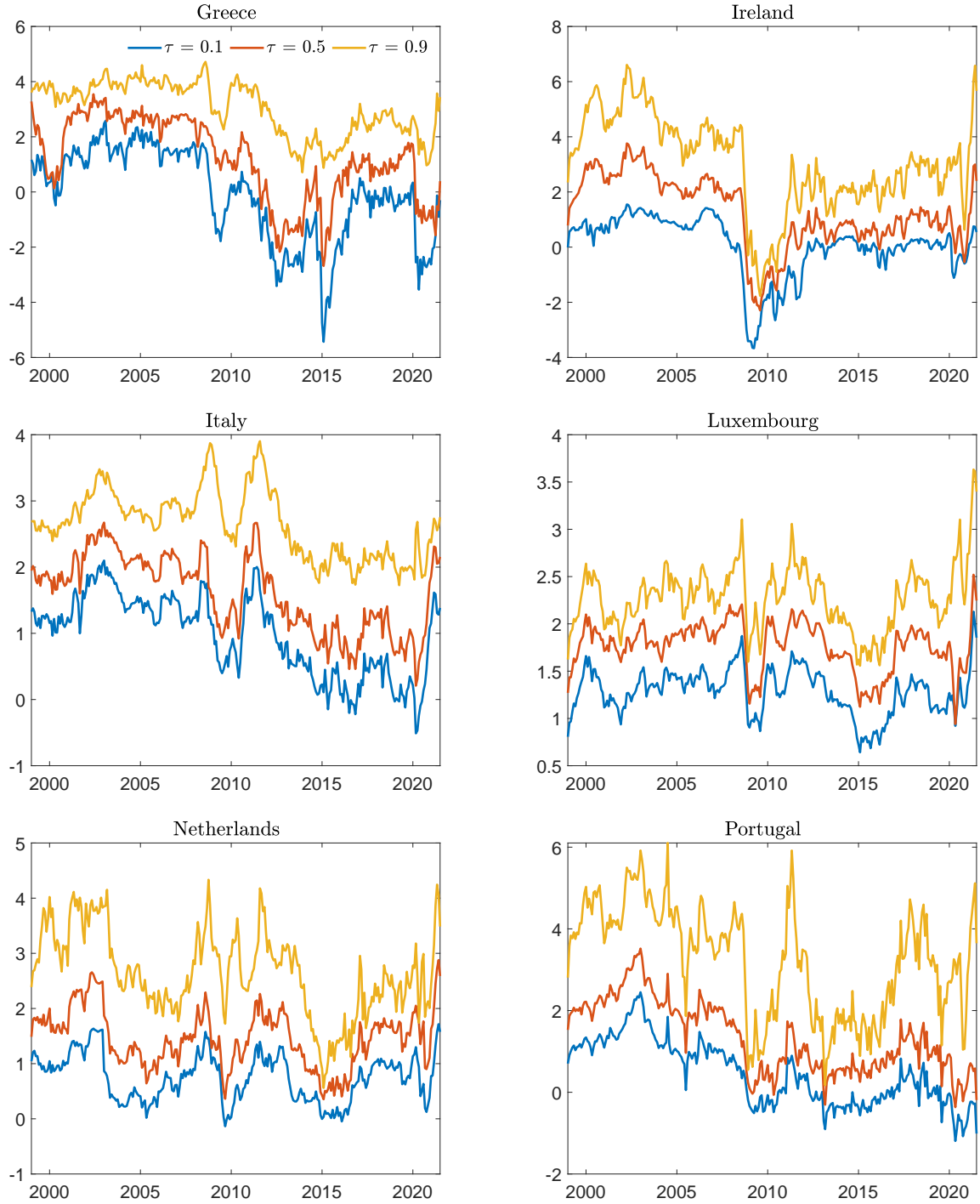
## APPENDIX D. CONDITIONAL QUANTILES, EXPECTED SHORTFALL AND LONGRISE

FIGURE D1. Conditional quantiles by country



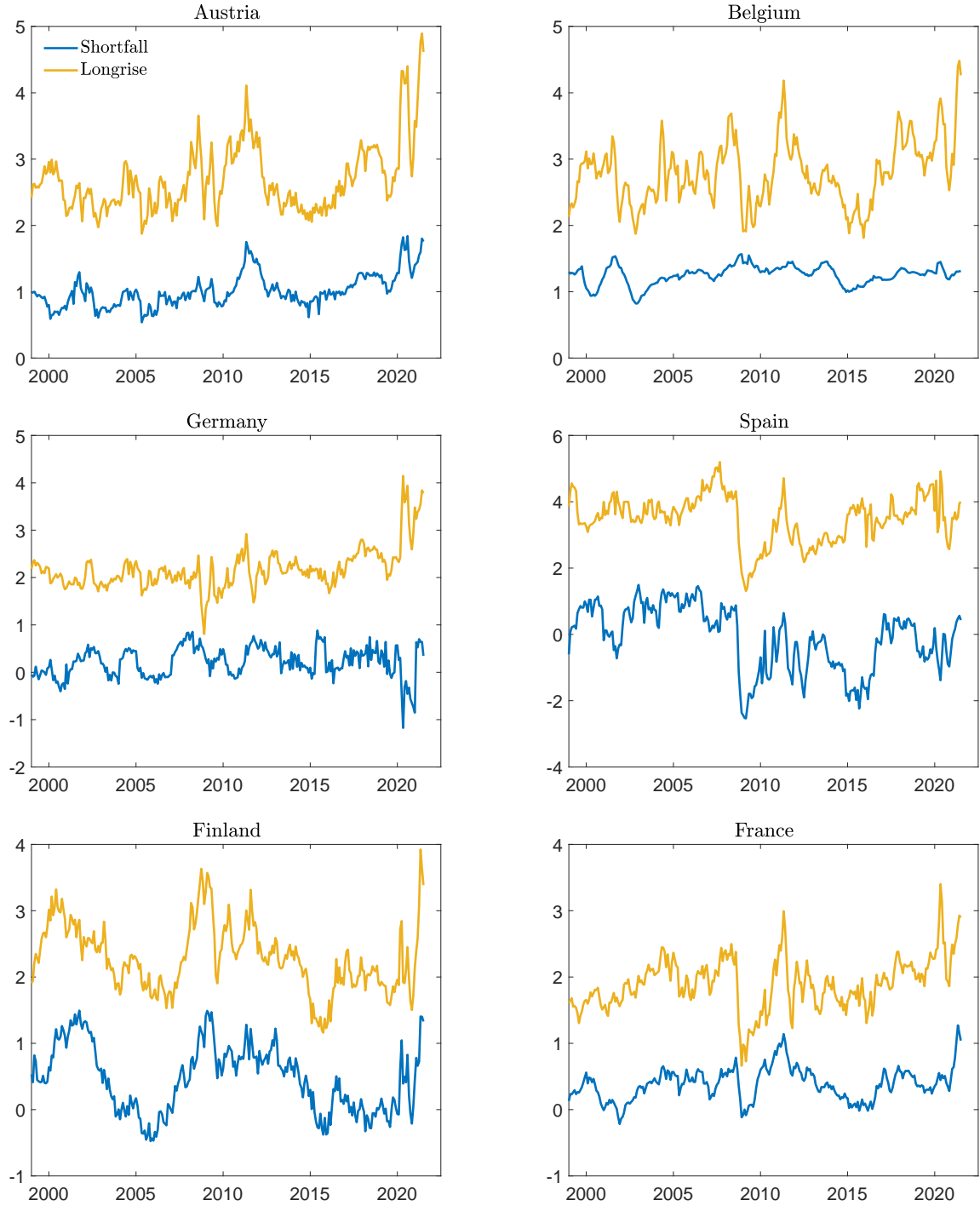
*Note:* Conditional inflation quantiles  $\hat{Q}_\tau(\bar{\pi}_{t+1,t+h}^i | x_t^i)$  for country  $i$ , quantiles  $\tau = \{0.1; 0.5; 0.9\}$  and forecast horizon  $h = 12$ . Conditional quantiles  $\hat{Q}_\tau(\bar{\pi}_{t+1,t+h}^i | x_t^i)$  are simulated using the estimates of Equation (2).

FIGURE D2. Conditional quantiles by country



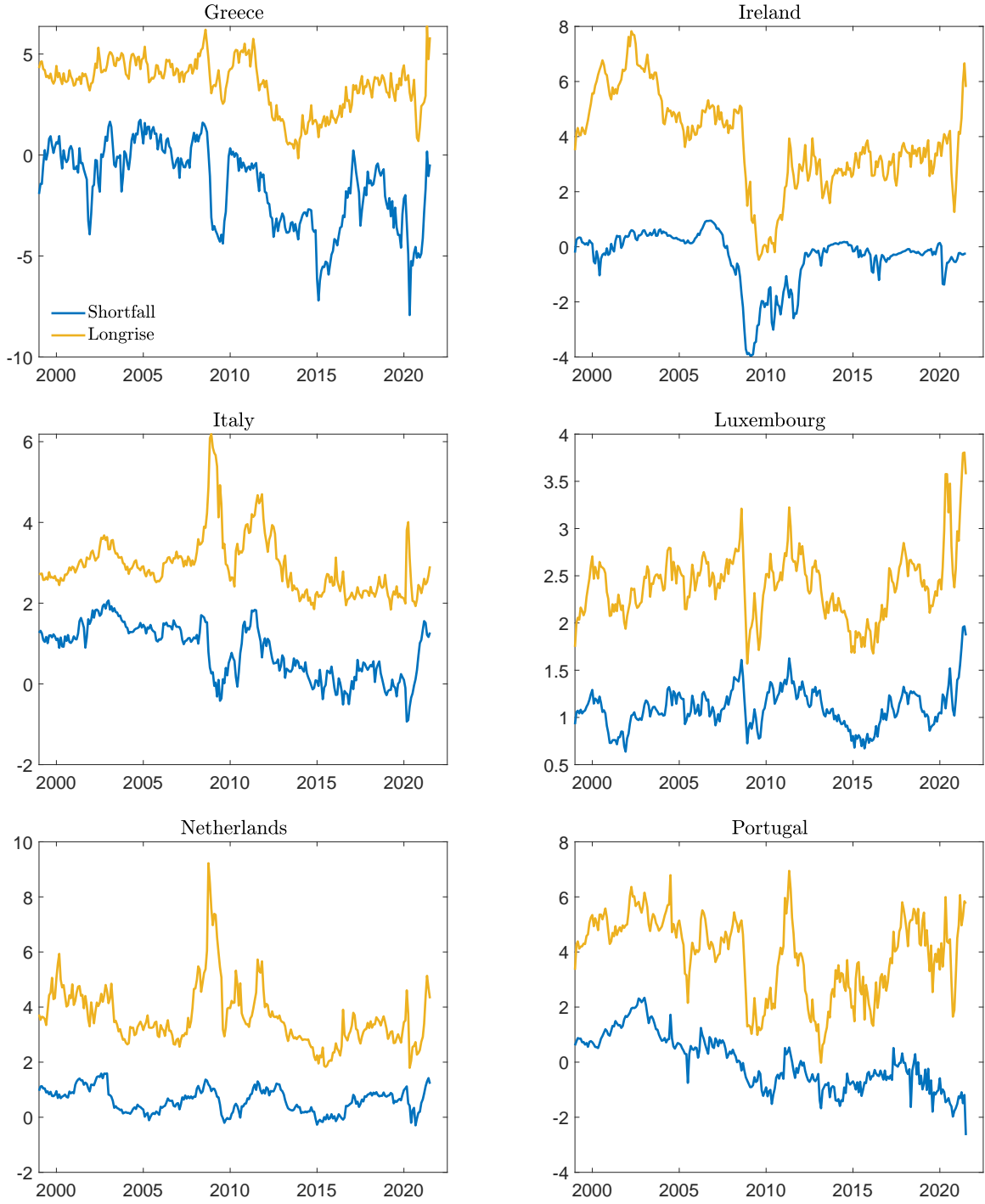
*Note:* Conditional inflation quantiles  $\hat{Q}_\tau(\bar{\pi}_{t+1,t+h}^i | x_t^i)$  for country  $i$ , quantiles  $\tau = \{0.1; 0.5; 0.9\}$  and forecast horizon  $h = 12$ . Conditional quantiles  $\hat{Q}_\tau(\bar{\pi}_{t+1,t+h}^i | x_t^i)$  are simulated using the estimates of Equation (2).

FIGURE D3. Expected shortfall and longrise by country



*Note:* Expected shortfall and longrise  $SF_{t+h}^i$  and  $LR_{t+h}^i$  for country  $i$ ,  $p = 0.10$  and forecast horizon  $h = 12$ .  $SF_{t+h}^i$  and  $LR_{t+h}^i$  are defined by Equation (6).

FIGURE D4. Expected shortfall and longrise by country



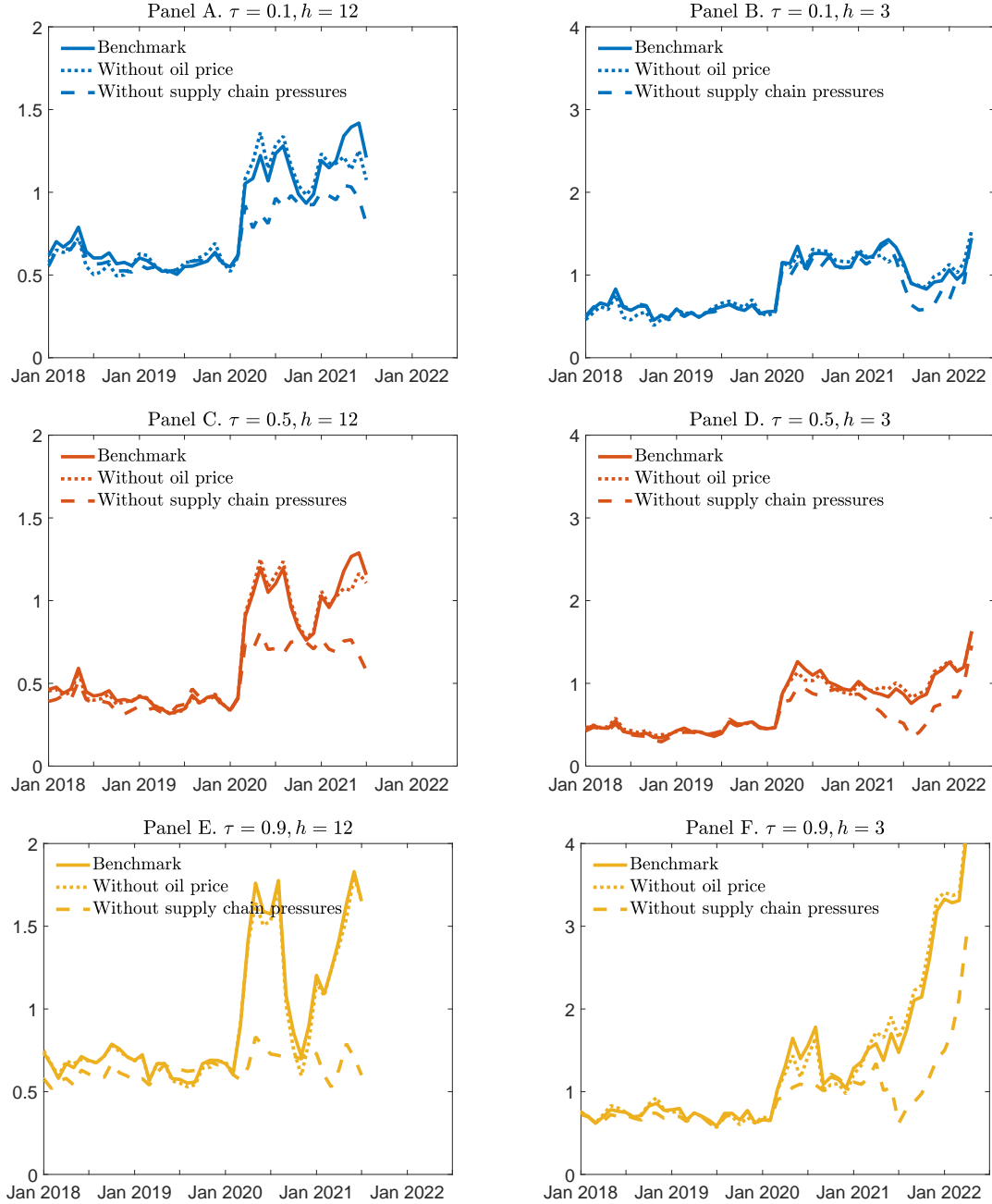
*Note:* Expected shortfall and longrise  $SF_{t+h}^i$  and  $LR_{t+h}^i$  for country  $i$ ,  $p = 0.10$  and forecast horizon  $h = 12$ .  $SF_{t+h}^i$  and  $LR_{t+h}^i$  are defined by Equation (6).

## APPENDIX E. COUNTERFACTUAL EXERCISES USING HICP

Figure E5 depicts the results using HICP instead of core HICP used in the benchmark model. Considering headline inflation in the analysis confirms previous results of the role of global supply chain in the evolution of inflation distribution. However, the results are even more striking than in the case where core inflation is used, especially regarding the results for  $h = 12$  and the 90<sup>th</sup> quantile (Panel E). The dispersion peaks around March 2020 and at the end of the sample period of estimation to reach levels almost thrice the one observed during the COVID crisis. However, without supply chain pressures, the dispersion of inflation at the top of the distribution would have been muted, or at least similar to the level observed before the pandemic outbreak. From this point of view, tensions on global supply chain is a more important feature of HICP dispersion than core inflation dispersion across euro area countries.

On the other hand, the results for  $h = 3$  and the 90<sup>th</sup> quantile (Panel F) contrast a little with the previous ones, at least regarding the last months of the estimation period. They suggest that supply chain pressures have played a less prominent role in inflation dispersion during the COVID crisis, and that this effect has been particularly decreasing over the last few months of the sample period. Simulated series without supply chain seems to catch up the dispersion series estimated with the benchmark model.

FIGURE E5. Dispersion of conditional quantiles without oil price and supply chain pressures (HICP inflation)



*Note:* The case without oil price corresponds to the standard deviation of conditional quantiles predicted for  $\pi_t^{o,*} = \pi_t^{*,i}$  in the quantile Phillips curve (2) estimated with HICP. The case without supply chain pressures corresponds to the standard deviation of conditional quantiles predicted for  $sc_t = 0$  in the quantile Phillips curve (2). The first column of panels is for the one-year forecast ( $h = 12$ ) and the second one is for the one-quarter forecast ( $h = 3$ ). The first row of panels is for the 10<sup>th</sup> quantile, the second one for the 50<sup>th</sup> quantile, and the third one for the 90<sup>th</sup> quantile.

## APPENDIX F. MARKOV-SWITCHING PROCEDURE

**F.1. The Posterior Density.** Since the posterior density function of Markov-switching models is very non-Gaussian, it is essential to find the posterior mode via an optimization routine prior to sample from the posterior density. The estimate of the mode not only represents the most likely value, but also serves as a crucial starting point for initializing different chains of Monte Carlo Markov Chains (MCMC) draws.

The strategy to find the posterior mode is to generate a sufficient number of draws from the prior distribution of each parameter. Each set of points is then used as starting points to the `CSMINWEL` program, the optimization routine developed by Christopher A. Sims. Starting the optimization process at different values allows us to correctly cover the parameter space and avoid getting stuck in a “local” peak. Note, however, that we do not need to use a more complicated method for finding the mode like the blockwise optimization method developed by [Sims, Waggoner, and Zha \(2008\)](#). The authors employ a class of richly parameterized multivariate Markov-switching models in which the parameters are break into several subblocks, and then apply a standard hill-climbing quasi-Newton optimization routine to each block, while keeping the other subblocks constant, in order to maximize the posterior density. The size of Markov-switching univariate models remains relatively small and allows us to employ a more standard technique.

The posterior density is not of standard form, making it impossible to sample directly from this probability distribution. One can, however, use the idea of Gibbs sampling to obtain the empirical joint posterior density by sampling alternately from the following conditional posterior distribution. Our Gibbs sampler procedure begins with setting parameters at the peak of the posterior density function. The MCMC sampling sequence involves a 4-block Gibbs sampler, in which we can generate in a flexible and straightforward manner alternatively draws from full conditional posterior distributions. Overall, our procedure follows the MCMC approach proposed by [Albert and Chib \(1993\)](#).

In the remainder of this section, we simplify the notation by suppressing the superscript  $i$  denoting the country of interest. For  $1 \leq k \leq H$ , let  $\theta(k) = [\mu(k), \lambda(k), \theta(k), \gamma(k), \delta(k), \phi(k)]'$ ,  $S_t = [s_1, \dots, s_t]$ , and  $q_k$  be the  $k$ -th column of  $Q$ . The objects  $\theta(k)$  and  $q_k$  are

vectors of parameters. The prior on the set of parameters is given by:

$$p(\theta(k)) = \text{normal}(\theta(k)|\bar{\theta}_1, \bar{\theta}_2), \quad (10)$$

$$p(\sigma(k)) = \text{inv-gamma}(\sigma(k)|\bar{\sigma}_1, \bar{\sigma}_2), \quad (11)$$

$$p(q_k) = \text{dirichlet}(q_k|\bar{q}_{1,k}, \bar{q}_{2,k}, \bar{q}_{3,k}), \quad (12)$$

where  $\bar{\theta}_1$ ,  $\bar{\theta}_2$ ,  $\bar{q}_{1,j}$ ,  $\bar{q}_{2,j}$ , and  $\bar{q}_{3,j}$  are the hyperparameters;  $\text{normal}(x|.)$  denotes the multivariate normal distribution;  $\text{inv-gamma}(x|.)$  denotes the inverse gamma distribution; and  $\text{dirichlet}(x|.)$  denotes the dirichlet distribution.

In our empirical setting, our normal prior for  $\theta(k)$  is very dispersed and cover a large parameter space. We choose a prior with the mean 0.00 and the standard deviation 5.00, except for the prior of  $\lambda(k)$ , of which the mean 0.50 and the standard deviation 0.20, and truncated to values between zero and one. The inverse-gamma prior for the scale parameter,  $\sigma(k)$ , are set as  $\bar{\sigma}_1 = 0.1938$  and  $\bar{\sigma}_2 = 2.1551$ . It may be worth noting that we impose the exact same prior across regimes and across countries, so that the differences in parameters between regimes and countries result more from data (i.e., the likelihood) rather than priors. We imply a prior belief that the average duration of staying in the same regime is about eleven months. This means that, for example, the hyperparameters are  $\bar{q}_{1,j} = 20$ ,  $\bar{q}_{2,j} = \bar{q}_{3,j} = 1$  for the first regime. See [Sims, Waggoner, and Zha \(2008\)](#) for further details on how to define prior beliefs about the persistence of the regimes.

The MCMC sampling scheme at the  $(n)$ st iteration, for  $n = 1, \dots, N_1 + N_2$ , consists of sampling from the following conditional posterior distributions

- (1)  $p\left(S_T^{(n)}|Y_T, \theta^{(n-1)}, Q^{(n-1)}\right),$
- (2)  $p\left(Q^{(n)}|S_T\right),$
- (3)  $p\left(\theta^{(n)}(k)|Y_T, S_T^{(n)}, \sigma^{(n-1)}\right),$
- (4)  $p\left(\sigma(k)^{(n)}|Y_T, S_T^{(n)}, \theta^{(n)}\right),$

where  $Y_t$  are observed data,  $\theta = \theta(k)_{k \in H}$ , and  $\sigma = \sigma(k)_{k \in H}$ . Simulation from the conditional posterior density  $p\left(S_T^{(n)}|Y_T, \theta^{(n-1)}\right)$ , given  $\theta$  and  $Q$ , is standard and in closed form. Simulation from the conditional posterior density  $p\left(Q^{(n)}|S_T\right)$  is of the dirichlet form. Simulations from the conditional posterior densities  $p\left(\theta^{(n)}(k)|Y_T, S_T^{(n)}, \sigma^{(n-1)}\right)$  and  $p\left(\sigma(k)^{(n)}|Y_T, S_T^{(n)}, \theta^{(n)}\right)$  reduces to Bayesian inference for Markov-switching models with known allocations,  $S_T$ .



The sampler begins with setting parameters at the peak of the posterior density function. We generate  $N_1 + N_2 = 11,000$  draws, the first  $N_1 = 1,000$  are discarded as burn-in and of the remaining  $N_2 = 10,000$  draws, one of every 10 draws is retained to get 1,000 draws of parameters and sequences of regimes.

We now provide further details on each of these conditional density functions. In the remainder of this section, we simplify the notation by suppressing the superscript  $n$  denoting the  $n$ -th draws of the simulation.

F.1.1. *Conditional posterior densities,  $p(S_T|Y_T, \theta, Q)$ .* Following the [Carter and Kohn \(1994\)](#)'s multi-move Gibbs-sampling procedure, one can stimulate  $S_T$  as a block. We begin with a draw from  $p(s_T|Y_T, \theta, Q)$  obtained with the [Hamilton \(1989\)](#) basic filter, and then iterate recursively backward to draw  $s_{T-1}, s_{T-2}, \dots, 1$  according to

$$p(s_t|Y_T, \theta, Q) = \sum_{s_{t+1} \in H} p(s_t|Y_t, \theta, Q, s_{t+1})p(s_{t+1}|Y_T, \theta, Q), \quad (13)$$

where

$$p(s_t|Y_t, \theta, Q, s_{t+1}) = \frac{q_{s_{t+1}, s_t} p(s_t|Y_t, \theta, Q)}{p(s_{t+1}|Y_t, \theta, Q)} \quad (14)$$

F.1.2. *Conditional posterior densities,  $p(Q|S_T)$ .* Given the historical path of regimes, the transition matrix can be directly simulate from the Dirichlet distribution. For each column  $k$  of  $Q$ , denoted  $q_k$ , the conditional posterior distribution is given by

$$p(q_k|S_T) = \text{dirichet}(q_k|\bar{q}_{1,k} + \eta_{1,k}, \bar{q}_{2,k} + \eta_{2,k}, \bar{q}_{3,k} + \eta_{3,k}), \quad (15)$$

where  $\bar{q}_{1,k}$ ,  $\bar{q}_{2,k}$  and  $\bar{q}_{3,k}$  are the parameters describing the prior, and  $\eta_{i,k}$  denotes the numbers of transitions from state  $k$  to state  $i$ .

F.1.3. *Conditional posterior densities,  $p(\theta(k)|Y_T, S_T, \sigma)$ .* [Geweke \(1996\)](#) implements a Gibbs sampling procedure for the problem of multiple linear regression with a set of independent inequality linear constraints. We follow a similar procedure for our Markov-switching model with known allocations  $S_T$ .

The Markov-switching model in (8) can be rewritten in a compact as  $y_t = \theta(s_t)'x_t + \sigma(s_t)\varepsilon_t$ , where  $y_t$  is our variable of interest, and  $x_t$  contains the vectors of observed data at date  $t$ . Let  $y_t^* = \frac{y_t}{\sigma_{s_t}}$ , and  $x_t^* = \frac{x_t}{\sigma_{s_t}}$ , we obtain an homoskedastic model as follows

$$y_t^* = \theta(s_t)'x_t^* + \nu_t, \quad (16)$$

where  $\nu_t$  follows a standard normal distribution. Then, simulation from the full conditional distribution of  $\Psi$ , given  $Y_T$ ,  $S_T$ , and  $\sigma$ , becomes straightforward, given a conjugate prior distribution. For  $1 \leq k \leq H$ , the posterior is defined as

$$p(\theta(k)|Y_T, S_T) = \text{truncated-normal}(\theta(k)|m_{\mu,k}, M_{\mu,k})_{a \leq \theta(k) \leq b}, \quad (17)$$

where  $\text{truncated-normal}(x|\bar{x}_1, \bar{x}_2)_{a \leq x \leq b}$  is the truncated multivariate normal distribution with mean  $\bar{x}_1$ , variance-covariance  $\bar{x}_2$ , and inequality constraints  $a \leq x \leq b$ . The vector  $m_{\mu,k}$  and matrix  $M_{\mu,k}$  are defined as follows

$$m_{\mu,k} = (\bar{\theta}_2^{-1} + \Sigma_{xx,k})^{-1} (\bar{\theta}_2^{-1} \bar{\theta}_1 + \Sigma_{xy,k}), \quad (18)$$

$$M_{\mu,k} = (\bar{\theta}_2^{-1} + \Sigma_{xx,k})^{-1}, \quad (19)$$

with  $\bar{\theta}_1$  and  $\bar{\theta}_2$  are known hyperparameters of the prior distribution, and

$$\Sigma_{xx,k} = \sum_{t \in \{t:s_t=k\}} x_t^* x_t^{*'},$$

$$\Sigma_{xy,k} = \sum_{t \in \{t:s_t=k\}} x_t^* y_t^*.$$

This step implies a computational complication that requires the simulation from a truncated multivariate normal distribution. We use the minimax tilting method proposed by Botev (2017) for exact independently and identically distributed data simulation from the truncated multivariate normal distribution.<sup>9</sup> The method is an excellent algorithm designed for extremely fast simulation.

F.1.4. *Conditional posterior densities,  $p(\sigma(k)|Y_T, S_T, \theta)$ .* Given  $Y_t$ ,  $S_T$ , and  $\theta$ , the scale parameter  $\sigma(k)$  can be drawn using the following inverse-gamma distribution

$$p(\sigma(k)|Y_T, S_T, \theta) = \text{inv-gamma}(\sigma(k)|\tilde{\alpha}, \tilde{\beta}), \quad (20)$$

where

$$\begin{aligned} \tilde{\alpha} &= \bar{\sigma}_1 + \sum_{t \in \{t:s_t=k\}} (y_t - \theta'_{s_t} x_t)^2, \\ \tilde{\beta} &= \bar{\sigma}_2 + T_k, \end{aligned}$$

---

<sup>9</sup>The Matlab function is available at <https://fr.mathworks.com/matlabcentral/fileexchange/53792-truncated-multivariate-normal-generator>.

with  $\sum_{t \in \{t: s_t = k\}} (y_t - \theta'_{s_t} x_t)^2$  is the sum of squared residual,  $T_k$  is the number of elements of  $t$ 's such that  $s_t = k$  for  $k = 1, 2, 3$ , and  $\bar{\sigma}_1$  and  $\bar{\sigma}_2$  are the hyperparameters.

**F.2. Additional Results.** Tables **F1**, **F2**, **F3** and **F4** reports the posterior distribution of parameters for each country.

TABLE F1. Posterior Distributions - Markov-switching framework

	$\mu^i(s_t = 1)$	$\lambda^i(s_t = 1)$	$\theta^i(s_t = 1)$	$\gamma^i(s_t = 1)$	$\delta^i(s_t = 1)$	$\phi^i(s_t = 1)$	$\sigma^i(s_t = 1)$
Germany	-1.09 [-1.35;-0.81]	0.46 [0.20;0.75]	-0.50 [-1.52;-0.05]	0.46 [0.10;0.84]	1.29 [-0.21;3.83]	0.16 [0.02;0.53]	0.33 [0.26;0.44]
France	-1.05 [-1.18;-0.90]	0.93 [0.78;0.99]	-0.07 [-0.22;-0.00]	0.15 [0.01;0.42]	-0.65 [-1.33;0.06]	0.11 [0.02;0.22]	0.21 [0.18;0.27]
Italy	-0.81 [-1.15;-0.43]	0.66 [0.33;0.94]	-0.11 [-0.31;-0.01]	0.13 [0.01;0.36]	0.29 [-1.17;1.38]	0.07 [0.01;0.24]	0.28 [0.22;0.33]
Spain	-1.78 [-2.05;-1.21]	0.90 [0.63;0.99]	-0.13 [-0.29;-0.01]	0.31 [0.03;0.86]	-0.56 [-2.38;0.32]	0.20 [0.04;0.40]	0.35 [0.26;0.50]
Netherlands	-0.93 [-1.07;-0.79]	0.89 [0.77;0.98]	-0.69 [-1.02;-0.30]	0.32 [0.07;0.62]	0.31 [-0.34;0.92]	0.18 [0.03;0.37]	0.30 [0.25;0.36]
Finland	-0.93 [-1.14;-0.70]	0.70 [0.49;0.89]	-0.12 [-0.27;-0.01]	0.12 [0.01;0.41]	0.56 [-1.23;2.00]	0.20 [0.03;0.38]	0.27 [0.23;0.32]
Ireland	-1.55 [-1.95;-1.28]	0.96 [0.87;1.00]	-0.04 [-0.14;-0.00]	0.09 [0.01;0.32]	-4.30 [-5.09;-3.38]	0.24 [0.02;0.55]	0.56 [0.47;0.68]
Austria	-0.62 [-0.82;-0.44]	0.81 [0.59;0.96]	-0.14 [-0.42;-0.01]	0.18 [0.02;0.55]	0.32 [-0.49;1.67]	0.25 [0.05;0.86]	0.27 [0.22;0.37]
Portugal	-0.79 [-1.01;-0.61]	0.48 [0.36;0.59]	-0.04 [-0.16;-0.00]	0.30 [0.05;0.69]	-1.01 [-1.64;-0.30]	0.04 [0.00;0.14]	0.54 [0.48;0.60]
Belgium	-0.54 [-0.86;-0.22]	0.81 [0.14;0.97]	-0.24 [-0.76;-0.03]	0.22 [0.02;0.42]	0.48 [-5.56;5.23]	0.14 [0.01;0.22]	0.21 [0.17;0.25]
Luxembourg	-0.47 [-0.65;-0.29]	0.86 [0.56;0.99]	-0.12 [-0.40;-0.01]	0.28 [0.05;0.56]	0.03 [-0.92;0.96]	0.16 [0.02;0.35]	0.24 [0.20;0.29]
Greece	-2.79 [-3.69;-1.96]	0.43 [0.04;0.99]	-0.10 [-0.38;-0.01]	1.99 [0.70;3.71]	0.17 [-5.26;3.82]	0.52 [0.08;1.10]	0.71 [0.51;1.03]
Mean	-1.11	0.74	-0.19	0.38	-0.26	0.19	0.36
Std. Dev.	0.65	0.19	0.20	0.52	1.41	0.12	0.16

*Note:* Posterior median of Phillips curve's parameters based on Equation (8):  $\bar{\pi}_{t+1,t+h}^i = \mu^i(s_t^i) + (1 - \lambda^i(s_t^i)) \pi_{t-1}^{*,i} + \lambda^i(s_t^i) \pi^{\text{LTE},i} + \theta^i(s_t^i) (u_t^i - u_t^{*,i}) + \gamma^i(s_t^i) (\pi_t^{o,*} - \pi_t^{*,i}) + \delta^i(s_t^i) f_t^i + \phi^i(s_t^i) s c_t + \sigma^i(s_t^i) \varepsilon_t^i$ . The 90% probability interval is indicated in brackets.

TABLE F2. Posterior Distributions - Markov-switching framework

	$\mu^i(s_t = 2)$	$\lambda^i(s_t = 2)$	$\theta^i(s_t = 2)$	$\gamma^i(s_t = 2)$	$\delta^i(s_t = 2)$	$\phi^i(s_t = 2)$	$\sigma^i(s_t = 2)$
Germany	−0.45 [−0.57;−0.33]	0.92 [0.77;0.99]	−0.43 [−0.71;−0.13]	0.24 [0.04;0.47]	−0.26 [−0.66;0.26]	0.19 [0.06;0.31]	0.27 [0.23;0.31]
France	−0.43 [−0.55;−0.28]	0.89 [0.76;0.98]	−0.30 [−0.55;−0.08]	0.11 [0.01;0.25]	−0.78 [−1.18;−0.35]	0.05 [0.01;0.16]	0.18 [0.15;0.22]
Italy	0.07 [−0.12;0.27]	0.76 [0.32;0.98]	−0.11 [−0.33;−0.01]	0.22 [0.04;0.50]	−0.35 [−1.66;1.42]	0.09 [0.01;0.22]	0.26 [0.20;0.32]
Spain	−0.27 [−0.42;−0.08]	0.50 [0.38;0.66]	−0.06 [−0.18;−0.01]	0.11 [0.01;0.53]	−0.21 [−0.98;0.69]	0.04 [0.03;0.14]	0.30 [0.25;0.36]
Netherlands	−0.18 [−0.43;0.01]	0.81 [0.63;0.96]	−0.91 [−1.49;−0.29]	0.36 [0.06;0.72]	0.35 [−1.01;2.85]	0.19 [0.03;0.59]	0.33 [0.25;0.45]
Finland	−0.04 [−0.20;0.10]	0.73 [0.39;0.94]	−0.13 [−0.31;−0.01]	0.44 [0.12;0.88]	0.51 [−0.12;4.89]	0.24 [0.05;0.48]	0.25 [0.20;0.31]
Ireland	−0.62 [−0.79;−0.45]	0.77 [0.67;0.89]	−0.08 [−0.26;−0.01]	0.41 [0.08;0.88]	−1.16 [−2.55;0.08]	0.10 [0.01;0.28]	0.38 [0.32;0.44]
Austria	−0.07 [−0.21;0.06]	0.91 [0.74;0.99]	−0.10 [−0.32;−0.01]	0.23 [0.04;0.48]	0.32 [−0.51;1.97]	0.22 [0.06;0.37]	0.23 [0.19;0.27]
Portugal	0.04 [−0.20;0.38]	0.33 [0.21;0.46]	−0.30 [−0.65;−0.05]	1.13 [0.86;1.40]	2.03 [0.55;3.12]	0.16 [0.02;0.42]	0.39 [0.33;0.45]
Belgium	0.03 [−0.51;0.42]	0.89 [0.70;0.99]	−0.19 [−0.62;−0.02]	0.12 [0.01;0.41]	0.12 [−1.48;1.07]	0.12 [0.02;0.54]	0.22 [0.18;0.29]
Luxembourg	0.08 [−0.06;0.20]	0.85 [0.69;0.98]	−0.22 [−0.49;−0.04]	0.24 [0.05;0.49]	−0.20 [−0.93;0.62]	0.04 [0.00;0.14]	0.18 [0.15;0.21]
Greece	−1.08 [−1.30;−0.81]	0.72 [0.58;0.93]	−0.48 [−0.74;−0.08]	0.19 [0.02;0.51]	0.64 [−0.67;1.84]	0.29 [0.05;0.54]	0.48 [0.37;0.57]
Mean	−0.24	0.76	−0.28	0.32	0.08	0.14	0.29
Std. Dev.	0.35	0.18	0.24	0.28	0.81	0.08	0.09

*Note:* Posterior median of Phillips curve's parameters based on Equation (8):  $\bar{\pi}_{t+1,t+h}^i = \mu^i(s_t^i) + (1 - \lambda^i(s_t^i)) \pi_{t-1}^{*,i} + \lambda^i(s_t^i) \pi^{\text{LTE},i} + \theta^i(s_t^i) (u_t^i - u_t^{*,i}) + \gamma^i(s_t^i) (\pi_t^{O,*} - \pi_t^{*,i}) + \delta^i(s_t^i) f_t^i + \phi^i(s_t^i) sc_t + \sigma^i(s_t^i) \varepsilon_t^i$ . The 90% probability interval is indicated in brackets.

TABLE F3. Posterior Distributions - Markov-switching framework

	$\mu^i(s_t = 3)$	$\lambda^i(s_t = 3)$	$\theta^i(s_t = 3)$	$\gamma^i(s_t = 3)$	$\delta^i(s_t = 3)$	$\phi^i(s_t = 3)$	$\sigma^i(s_t = 3)$
Germany	0.65 [0.41;0.95]	0.91 [0.71;0.99]	-0.15 [-0.65;-0.01]	0.21 [0.02;0.69]	-2.67 [-4.17;-0.79]	0.37 [0.19;0.56]	0.48 [0.38;0.62]
France	0.17 [0.02;0.33]	0.84 [0.61;0.98]	-0.57 [-0.93;-0.20]	0.13 [0.01;0.36]	-0.87 [-3.02;1.43]	0.30 [0.19;0.42]	0.21 [0.18;0.26]
Italy	0.78 [0.53;1.07]	0.58 [0.25;0.87]	-0.22 [-0.75;-0.03]	0.21 [0.02;0.59]	0.75 [-0.93;2.78]	0.08 [0.00;0.30]	0.33 [0.25;0.41]
Spain	0.97 [0.73;1.23]	0.90 [0.69;0.99]	-0.73 [-1.06;-0.41]	0.11 [0.01;0.39]	-2.55 [-3.82;-1.15]	0.45 [0.25;0.70]	0.44 [0.35;0.53]
Netherlands	1.24 [0.82;1.92]	0.91 [0.68;0.99]	-1.16 [-2.29;-0.37]	1.11 [0.40;1.70]	-0.17 [-2.85;3.35]	0.08 [0.01;0.30]	0.57 [0.40;0.73]
Finland	0.31 [0.01;0.81]	0.56 [0.18;0.89]	-0.18 [-0.51;-0.02]	0.73 [0.21;1.13]	1.42 [-1.06;4.59]	0.39 [0.13;0.57]	0.27 [0.21;0.36]
Ireland	1.68 [1.21;2.18]	0.68 [0.52;0.86]	-0.65 [-1.21;-0.16]	0.16 [0.02;0.53]	0.67 [-4.09;5.03]	0.71 [0.41;1.02]	0.84 [0.73;0.98]
Austria	0.61 [0.28;0.92]	0.80 [0.34;0.98]	-0.20 [-0.58;-0.02]	0.47 [0.10;0.95]	0.39 [-0.92;1.96]	0.60 [0.32;0.81]	0.30 [0.23;0.38]
Portugal	2.06 [1.62;2.51]	0.72 [0.29;0.96]	-2.02 [-2.89;-1.00]	1.54 [0.70;2.26]	0.66 [-4.27;5.26]	0.43 [0.08;1.01]	0.52 [0.39;0.71]
Belgium	0.64 [0.40;1.26]	0.87 [0.28;0.99]	-0.49 [-0.84;-0.10]	0.37 [0.05;0.90]	-0.36 [-2.20;1.48]	0.31 [0.07;0.52]	0.33 [0.24;0.42]
Luxembourg	0.63 [0.29;1.00]	0.59 [0.26;0.89]	-0.32 [-0.87;-0.03]	0.26 [0.03;0.64]	-0.30 [-2.89;2.00]	0.40 [0.24;0.55]	0.28 [0.20;0.40]
Greece	0.48 [0.21;0.73]	0.87 [0.73;0.97]	-0.35 [-0.70;-0.06]	0.66 [0.27;1.03]	1.55 [-0.26;3.65]	0.33 [0.03;0.65]	0.58 [0.49;0.67]
Mean	0.85	0.77	-0.59	0.50	-0.12	0.37	0.43
Std. Dev.	0.56	0.14	0.54	0.45	1.36	0.18	0.18

*Note:* Posterior median of Phillips curve's parameters based on Equation (8):  $\bar{\pi}_{t+1,t+h}^i = \mu^i(s_t^i) + (1 - \lambda^i(s_t^i)) \pi_{t-1}^{*,i} + \lambda^i(s_t^i) \pi^{\text{LTE},i} + \theta^i(s_t^i) (u_t^i - u_t^{*,i}) + \gamma^i(s_t^i) (\pi_t^{O,*} - \pi_t^{*,i}) + \delta^i(s_t^i) f_t^i + \phi^i(s_t^i) sc_t + \sigma^i(s_t^i) \varepsilon_t^i$ . The 90% probability interval is indicated in brackets.

TABLE F4. Posterior Distributions - Transition Matrices

	$q_{11}^i$	$q_{21}^i$	$q_{31}^i$	$q_{12}^i$	$q_{22}^i$	$q_{32}^i$	$q_{13}^i$	$q_{23}^i$	$q_{33}^i$
Germany	0.87 [0.80;0.93]	0.08 [0.03;0.15]	0.04 [0.01;0.10]	0.04 [0.02;0.07]	0.93 [0.88;0.96]	0.03 [0.01;0.07]	0.03 [0.01;0.07]	0.08 [0.04;0.15]	0.89 [0.82;0.94]
France	0.92 [0.85;0.96]	0.05 [0.01;0.11]	0.03 [0.01;0.08]	0.06 [0.02;0.13]	0.89 [0.80;0.94]	0.05 [0.02;0.12]	0.02 [0.00;0.07]	0.05 [0.01;0.10]	0.92 [0.87;0.96]
Italy	0.94 [0.89;0.98]	0.04 [0.01;0.09]	0.02 [0.00;0.04]	0.04 [0.02;0.10]	0.91 [0.84;0.95]	0.05 [0.02;0.09]	0.02 [0.00;0.06]	0.07 [0.03;0.13]	0.90 [0.84;0.95]
Spain	0.89 [0.82;0.94]	0.07 [0.03;0.14]	0.03 [0.01;0.09]	0.03 [0.01;0.06]	0.92 [0.88;0.96]	0.04 [0.02;0.08]	0.03 [0.01;0.07]	0.07 [0.03;0.13]	0.90 [0.84;0.95]
Netherlands	0.92 [0.87;0.95]	0.07 [0.03;0.11]	0.02 [0.00;0.04]	0.07 [0.03;0.12]	0.89 [0.83;0.94]	0.04 [0.01;0.09]	0.03 [0.01;0.09]	0.06 [0.02;0.12]	0.90 [0.83;0.96]
Finland	0.95 [0.91;0.98]	0.03 [0.01;0.06]	0.02 [0.00;0.05]	0.04 [0.01;0.08]	0.91 [0.84;0.95]	0.05 [0.02;0.11]	0.03 [0.01;0.08]	0.07 [0.03;0.13]	0.90 [0.82;0.95]
Ireland	0.91 [0.85;0.96]	0.06 [0.02;0.12]	0.02 [0.00;0.06]	0.04 [0.02;0.08]	0.93 [0.89;0.96]	0.02 [0.01;0.05]	0.02 [0.00;0.05]	0.04 [0.02;0.08]	0.94 [0.89;0.97]
Austria	0.88 [0.82;0.94]	0.09 [0.04;0.15]	0.03 [0.01;0.08]	0.05 [0.02;0.08]	0.90 [0.84;0.94]	0.05 [0.02;0.10]	0.02 [0.00;0.07]	0.09 [0.04;0.16]	0.88 [0.80;0.93]
Portugal	0.94 [0.90;0.97]	0.04 [0.01;0.07]	0.02 [0.00;0.04]	0.05 [0.02;0.09]	0.92 [0.88;0.96]	0.02 [0.01;0.05]	0.04 [0.01;0.10]	0.06 [0.02;0.13]	0.90 [0.81;0.96]
Belgium	0.91 [0.75;0.96]	0.06 [0.02;0.15]	0.03 [0.00;0.15]	0.06 [0.00;0.14]	0.89 [0.78;0.96]	0.06 [0.03;0.11]	0.02 [0.00;0.08]	0.08 [0.04;0.16]	0.89 [0.80;0.94]
Luxembourg	0.92 [0.88;0.96]	0.05 [0.02;0.10]	0.02 [0.00;0.06]	0.04 [0.02;0.08]	0.92 [0.88;0.96]	0.03 [0.01;0.07]	0.03 [0.01;0.09]	0.08 [0.03;0.16]	0.88 [0.79;0.94]
Greece	0.92 [0.86;0.96]	0.05 [0.02;0.11]	0.02 [0.01;0.07]	0.03 [0.01;0.07]	0.92 [0.88;0.96]	0.04 [0.02;0.08]	0.01 [0.00;0.04]	0.03 [0.01;0.06]	0.95 [0.92;0.98]

*Note:* Posterior median of transition matrices. The 90% probability interval is indicated in brackets.